Protist, Vol. 162, 738–761, November 2011
http://www.elsevier.de/protis
Published online date 28 June 2011

Protist

ORIGINAL PAPER

Integrative Taxonomy of the Pavlovophyceae (Haptophyta): A Reassessment

El Mahdi Bendif[a,b,1], Ian Probert[a,2], Annie Hervé[c], Chantal Billard[b], Didier Goux[d], Christophe Lelong[b], Jean-Paul Cadoret[c], and Benoît Véron[a,b,3]

[a]Université de Caen Basse-Normandie, Algobank-Caen, IFR 146, 14032 Caen, France
[b]Université de Caen Basse-Normandie, UMR 100 PE2 M - IFREMER, 14032 Caen, France
[c]IFREMER, Laboratoire de Physiologie et Biotechnologie des Algues, rue de l'Ile d'Yeu, BP21105, 44311 Nantes, France
[d]Université de Caen Basse-Normandie, Centre de Microscopie Appliquée à la Biologie, IFR 146, 14032 Caen, France

Submitted October 18, 2010; Accepted March 15, 2011
Monitoring Editor: Barry S. C. Leadbeater.

The Pavlovophyceae (Haptophyta) contains four genera (*Pavlova*, *Diacronema*, *Exanthemachrysis* and *Rebecca*) and only thirteen characterised species, several of which are important in ecological and economic contexts. We have constructed molecular phylogenies inferred from sequencing of ribosomal gene markers with comprehensive coverage of the described diversity, using type strains when available, together with additional cultured strains. The morphology and ultrastructure of 12 of the described species was also re-examined and the pigment signatures of many culture strains were determined. The molecular analysis revealed that sequences of all described species differed, although those of *Pavlova gyrans* and *P. pinguis* were nearly identical, these potentially forming a single cryptic species complex. Four well-delineated genetic clades were identified, one of which included species of both *Pavlova* and *Diacronema*. Unique combinations of morphological/ultrastructural characters were identified for each of these clades. The ancestral pigment signature of the Pavlovophyceae consisted of a basic set of pigments plus MV chl cPAV, the latter being entirely absent in the *Pavlova* + *Diacronema* clade and supplemented by DV chl cPAV in part of the *Exanthemachrysis* clade. Based on this combination of characters, we propose a taxonomic revision of the class, with transfer of several *Pavlova* species to an emended *Diacronema* genus. The evolution of the class is discussed in the context of the phylogenetic reconstruction presented.

Key words: 18S rDNA; Haptophyta; Pavlovophyceae; phylogeny; taxonomy; ultrastructure.

Introduction

The Haptophyta is a phylum of chlorophyll a + c containing unicellular algae characterised by the presence of a unique filamentous appendage, the haptonema, and comprising two distinct classes, the Prymnesiophyceae Hibberd emend. Cavalier-Smith and the Pavlovophyceae (Cavalier-Smith) Green et Medlin. The erection of a third class of

[1]Present address: CNRS-UMPC (Université Paris-06), UMR 7144, Groupe Plancton, Station Biologique de Roscoff, BP74, 29682 Roscoff cedex, France
[2]Present address: Roscoff Culture Collection, CNRS-UMPC (Université Paris-06), FR2424, Station Biologique de Roscoff, BP74, 29682 Roscoff cedex, France
[3]Corresponding author; fax +33 2 31 56 53 46
e-mail benoit.veron@unicaen.fr (B. Véron).

doi:10.1016/j.protis.2011.05.001

haptophytes was recently proposed based exclusively on molecular data (Shi et al. 2009). The Prymnesiophyceae contains ca. 400 described species including many well known taxa such as *Phaeocystis*, *Chrysochromulina*, *Prymnesium* and the coccolithophores that can periodically form blooms in coastal and oceanic environments and thereby have a highly visible impact on marine ecosystem functioning, global biogeochemical cycles and global climate change (Moestrup 1994). By contrast, the Pavlovophyceae contains only 13 described species that inhabit littoral, brackish water and sometimes freshwater environments, and which have consequently not received a great deal of attention in the context of global issues.

The Pavlovophyceae is nevertheless a class of interest for a number of reasons, not least because it is seemingly a very common component of near coastal phytoplankton communities in widespread locations. The Pavlovophyceae synthesize long chain polyunsaturated fatty acids such as docosahexaenoic (DHA) and eicosapentaenoic (EPA) acids and certain species, notably *Pavlova lutheri* and *P. gyrans*, are extensively used as feedstocks in the aquaculture of bivalves, crustaceans and fish (Gayral 1980; Green 1975; Meireles et al. 2003; Ponis et al. 2006). The separation of the two known haptophyte classes is genetically well supported with 6% divergence in 18S rDNA phylogeny (Edvardsen et al. 2000). Using molecular clocks calibrated with the coccolithophore fossil record, the time of divergence of these two classes of the Haptophyta has been estimated at between 805 and 1000 million years ago (de Vargas et al. 2007; Liu et al. 2010; Medlin et al. 2008). This deep divergence provides a model of key interest for evolutionary studies on the origin of the Haptophyta and the early radiation of eukaryotes.

In this context, the Pavlovophyceae are generally perceived to be representative of the primitive state, with characteristics likely to be related to those of the ancestral haptophyte. Structural features common to all or most members of the Pavlovophyceae that distinguish them from the Prymnesiophyceae include the markedly anisokont nature of the heterodynamic flagella and the relatively simple arrangement of microtubular and fibrous roots of the pavlovophycean flagellar-haptonematal basal complex (Green and Hori 1994). This flagellar arrangement results in pavlovophycean cells exhibiting a characteristic swimming movement. In addition, pavlovophycean scales, when present, consist of small dense bodies in contrast to the plate scales of the Prymnesiophyceae. These so-called 'knob scales', considered to be modified scales (Green 1980) or modified hairs (Cavalier-Smith 1994), often form a dense investment on the longer flagellum together with fine hairs. The process of mitosis in the Pavlovophyceae differs notably from that in the Prymnesiophyceae (Green and Hori 1988; Hori and Green 1994). The Pavlovophyceae are also known to synthesise certain specific sterols and conjugates, the pavlovols (Véron et al. 1996; Volkman et al. 1997) and a unique photosynthetic pigment (Van Lenning et al. 2003).

Due to their trophic, economic and phylogenetic importance, the Pavlovophyceae represent a highly relevant model for genomic studies. *Pavlova lutheri* was part of the protist EST program (http://megasun.bch.umontreal.ca/pepdb/pep.html, Tonon et al. 2005) and the genome size and structure of two species, *P. gyrans* and *Diacronema sp.*, have been estimated using Pulse Field Gel Electrophoresis with a view to the possibility of initiating a full genome sequencing project (Nosenko et al. 2007).

The 13 described species of Pavlovophyceae are classified in a single subclass, the Pavlovophycideae Cavalier-Smith, one order, the Pavlovales Green, and one family, the Pavlovaceae Green, that is composed of 4 genera: *Diacronema* (Prauser) Green et Hibberd, *Exanthemachrysis* Lepailleur, *Pavlova* (Butcher) Green and *Rebecca* Green (Table 1). Butcher (1952) erected the genus *Pavlova* with the description of *P. gyrans* as the type species. Based mostly on TEM ultrastructural studies of culture strains, new species were sporadically described until 1992. The last major taxonomic survey of the class was conducted over a quarter of a century ago (Green 1980), when a determination key was proposed for the three existing genera, *Diacronema*, *Pavlova* and *Exanthemachrysis*. More recently, the availability of 18S rDNA sequences for a sub-set of pavlovophycean taxa led to the transfer of two *Pavlova* species to the new genus *Rebecca* (Edvardsen et al. 2000). In addition, analysis of photosynthetic pigment profiles of a selection of species demonstrated that such profiles are phylogenetically informative (Van Lenning et al. 2003). In both of these latter studies, however, a complete reinvestigation of the class was not carried out. Undescribed species are frequently observed in miscellaneous samples (Gayral 1980) and the majority of the main microalgal culture collections hold several unidentified Pavlovophyceae strains that are likely to include new species.

Using type cultures when still available (11 of the 13 described species), we conducted a combined morphological, pigmentary and molecular genetic analysis in order to assess the validity of the current

Table 1. Actual Pavlovophyceae taxonomy and authorities.

Haptophyta Hibberd Cavalier-Smith ex Edvardsen et Eikrem in Edvardsen et al. 2000
Pavlovophyceae Cavalier-Smith ex Green et Medlin in Edvardsen et al. 2000
Pavlovales Green 1976
Pavlovaceae Green 1976
Diacronema (Prauser) Green et Hibberd 1977
Diacronema vlkianum (Prauser) Green et Hibberd 1977
Exanthemachrysis Lepailleur 1970
Exanthemachrysis gayraliae Lepailleur 1970
Pavlova Butcher 1952
Pavlova calceolata van der Veer 1976
Pavlova ennorea van der Veer et Leewis 1977
Pavlova granifera (Mack) Green 1973
Pavlova gyrans (Butcher) Green et Manton 1970
Pavlova lutheri (Droop) Green 1975
Pavlova noctivaga (Kalina 1970) van der Veer et Leewis 1977
Pavlova pinguis Green 1967
Pavlova virescens Billard 1976
Pavlova viridis Tseng, Chen et Zhang 1992
Rebecca Green 2000
Rebecca helicata (van der Veer) Green 2000
Rebecca salina (Carter) Green 2000

taxonomic scheme and to provide detailed information on phylogenetic relationships across the entire described diversity of the class. This led to a taxonomic revision of the class that will provide a framework for future description of the underestimated diversity within this lineage.

Results

Molecular Phylogenies

The twenty-eight 18S and twenty-seven 28S rDNA sequences of Pavlovophyceae generated in this study were added to 33 sequences from Genbank for the phylogenetic analyses. The accession numbers of these sequences are given in Table 2.

Phylogenetic trees generated for both genes and the concatenation using different methods (ML, Bayesian) recovered similar topologies, delineating four well-supported clades (Figs 1, 2 and 3). The sequence of the type strain of *Exanthemachrysis gayraliae* together with sequences of undescribed strains forms a first clade with a bootstrap value of 77%, 98% and 100%. Support for this branch is reinforced by the Bayesian posterior probability of 0.99, 1.00 and 1.00. A second, strongly supported clade (bootstrap value 100% posterior probability 1.00 [in all inferred trees]) is composed of the sequence of the type strain of *Rebecca* together with sequences of undescribed strains. The third and fourth clades split the genus *Pavlova*. The third clade (bootstrap value 96%, 80% and 89%, and posterior probability 1.00, 0.90 and 0.99), including sequences of the type strains of *P. gyrans*, *P. pinguis* and *P. granifera* and other unidentified *Pavlova* strains, splits into two well-supported subclades. The type strains of *P. gyrans* and *P. pinguis* have identical sequences, falling in a sub-clade with closely related sequences from other strains (mostly previously identified as *P. gyrans*, but some identified as *P. lutheri* or *Rebecca salina*). The other sub-clade includes sequences of the type strain of *P. granifera* and of several strains identified as *P. pinguis* as well as unidentified strains. The last clade, supported by an 87%, 58% and 97% bootstrap value with 1.00, 0.96 and 1.00 posterior probability, comprises a mix of distinct sequences of *Pavlova* and *Diacronema*.

Pigment Analyses

The suite of photosynthetic pigments identified across the *Pavlovophyceae* was identical to that reported by Van Lenning et al. (2003). No trace of 19′-hexanoyloxyfucoxanthin (HFx), 4-keto-hexanoyloxyfucoxanthin (4-keto-HFx), 4-keto-fucoxanthin (4-keto-Fx), monovinyl (MV), and divinyl (DV) forms of chl c3 or nonpolar chl c2 types were found in the strains analysed, confirming the conclusion of Van Lenning et al. (2003) that these compounds can be classified within the Haptophyta as typical pigments of the class

Table 2. Taxa with their original names and strains, genes and accession numbers used in the phylogenies (Figs 1, 2 and 3) (AC, Algobank-Caen www.unicaen.fr/algobank; ACOI, Coimbra culture collection http://acoi.ci.uc.pt; ASIO, Algal culture collection; CCAP, Culture Collection of Algae and Protozoa www.ccap.ac.uk; PLY, Plymouth Algal Culture Collection www.mba.ac.uk/culturecollection.php; SAG, SAG Culture collection http://sagdb.uni-goettingen.de).

Taxon	Strain Code	18SrDNA	28S rDNA	Pigment analysis
Diacronema vlkianum	AC67	JF714241	JF718748	x
*Exanthemachrysis gayraliae**	AC15	DQ531625	JF718765	x
*Pavlova ennorea**	AC253	JF714242	JF718754	x
*Pavlova granifera**	PLY552	JF714231	JF718774	x
Pavlova granifera	ACOI449	JF714243	JF718755	x
*Pavlova gyrans**	CCAP940/1b	JF714246	JF718771	x
*Pavlova lutheri**	PLY75	JF714236	JF718752	x
*Pavlova noctivaga**	SAG 5.83	JF714222	JF718756	x
*Pavlova pinguis**	CCAP940/2	JF714247	JF718769	x
*Pavlova virescens**	AC16	JF714235	JF718753	x
*Pavlova viridis**	ASIO3012	DQ075201		
Pavlova sp	AC19	JF714233	JF718757	x
Pavlova sp	AC28	JF714249	JF718772	x
Pavlova sp	AC33	JF714229	JF718761	x
Pavlova sp	AC35	JF714227	JF718767	x
Pavlova sp	AC37	JF714224	JF718766	x
Pavlova sp	AC54	JF714240	JF718749	x
Pavlova sp	AC245	JF714228	JF718768	x
Pavlova sp	AC246	JF714225	JF718753	x
Pavlova sp	AC247	JF714239	JF718750	x
Pavlova sp	AC248	JF714234	JF718759	x
Pavlova sp	AC249	JF714226	JF718762	x
Pavlova sp	AC250	JF714232	JF718758	x
Pavlova sp	AC251	JF714230	JF718760	x
Pavlova sp	AC252	JF714223	JF718764	x
Pavlova sp	AC537	JF714245	JF718773	x
Pavlova sp	AC538	JF714238	JF718751	x
*Rebecca salina**	PLY465	JF714244		
Rebecca salina	CCAP 940/3	JF714248	JF718768	x

*type strain

Prymnesiophyceae. In terms of pigment content, the profiles of all strains fell into the three pigment types (A, B and C) defined and detailed by Van Lenning et al. (2003). Type strains with pigment type A (the simplest pigment profile comprising Chls a, Mg-divinyl protochlorophyllide (MgDVP), c1, and c2 and the carotenoids fucoxanthin (Fx), diadinoxanthin (Ddx), diatoxanthin (Dtx), and ß-carotene) included *P. lutheri*, *P. virescens*, *P. noctivaga*, *P. ennorea* and *D. vlkianum*. Pigment type B (type A pigments plus an unknown Ddx-like carotenoid - Unk-1- and an unidentified DV form of chl c - DV-chl cPAV) was found in the type strains of *P. gyrans*, *P. pinguis* and *P. granifera*. Pigment type C (type B pigments plus MV-chl cPAV, the most complex composition observed) was restricted to the type strain of *E. gayraliae* and 2 other strains (AC37 and AC252). The superposition of pigment groupings and molecular phylogeny is shown in Figure 1.

Morphology and Ultrastructure

Pavlovophyceae cells are solitary or may form non-motile aggregations. Solitary cells are laterally flattened and typically highly metabolic. The anisokont flagella, when present, are inserted subapically or sometimes ventrally, and surround a non-coiling, often vestigial, haptonema. Flagellar movement is markedly heterodynamic. Intracellular storage bodies are present in some species, likely containing paramylon-like storage carbohy-

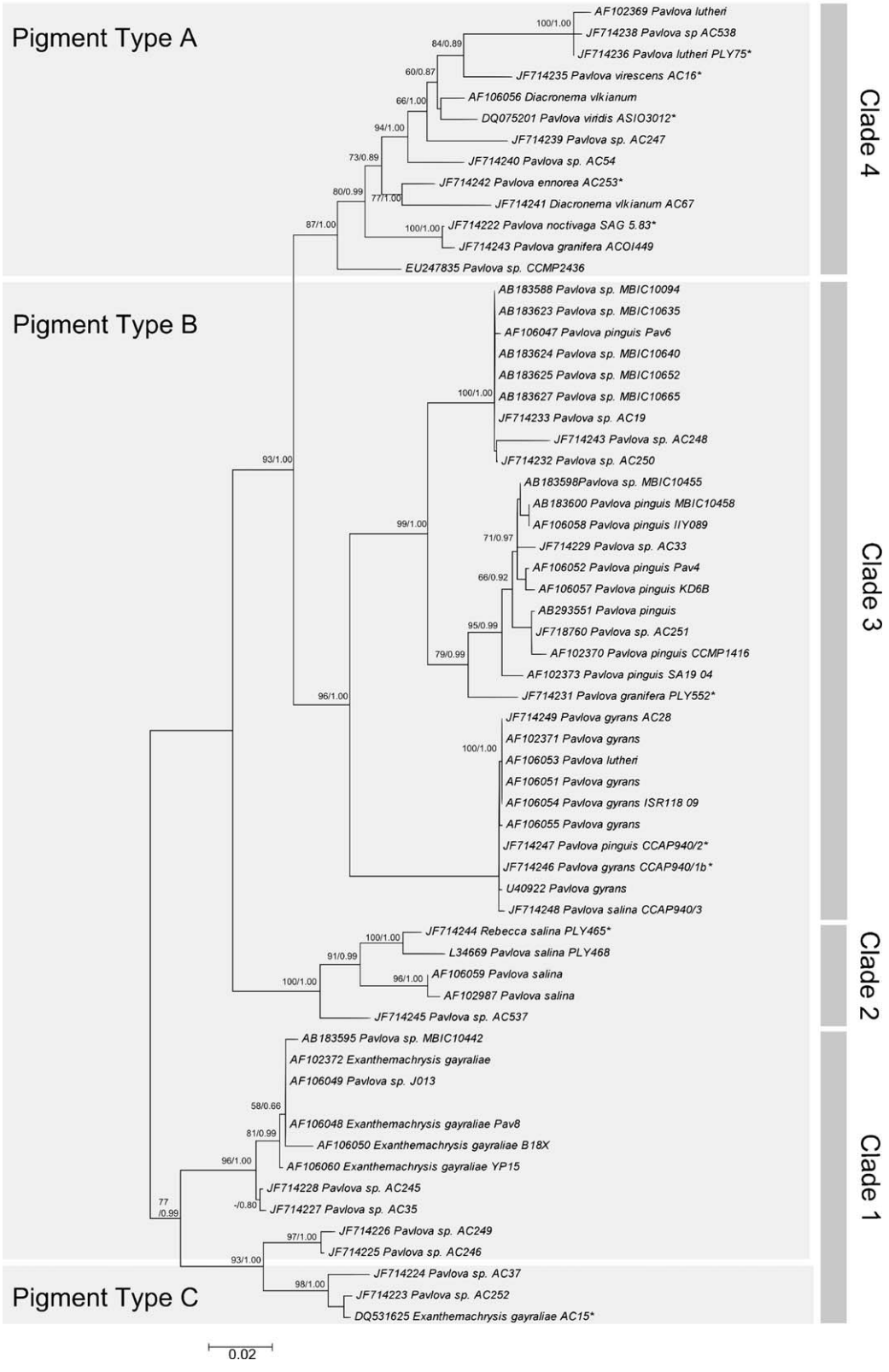
Pigment Type A
Pigment Type B
Pigment Type C
Clade 4
Clade 3
Clade 2
Clade 1
AF102369 Pavlova lutheri
JF714238 Pavlova sp AC538
JF714236 Pavlova lutheri PLY75*
JF714235 Pavlova virescens AC16*
AF106056 Diacronema vlkianum
DQ075201 Pavlova viridis ASIO3012*
JF714239 Pavlova sp. AC247
JF714240 Pavlova sp. AC54
JF714242 Pavlova ennorea AC253*
JF714241 Diacronema vlkianum AC67
JF714222 Pavlova noctivaga SAG 5.83*
JF714243 Pavlova granifera ACOI449
EU247835 Pavlova sp. CCMP2436
AB183588 Pavlova sp. MBIC10094
AB183623 Pavlova sp. MBIC10635
AF106047 Pavlova pinguis Pav6
AB183624 Pavlova sp. MBIC10640
AB183625 Pavlova sp. MBIC10652
AB183627 Pavlova sp. MBIC10665
JF714233 Pavlova sp. AC19
JF714243 Pavlova sp. AC248
JF714232 Pavlova sp. AC250
AB183598Pavlova sp. MBIC10455
AB183600 Pavlova pinguis MBIC10458
AF106058 Pavlova pinguis IIY089
JF714229 Pavlova sp. AC33
AF106052 Pavlova pinguis Pav4
AF106057 Pavlova pinguis KD6B
AB293551 Pavlova pinguis
JF718760 Pavlova sp. AC251
AF102370 Pavlova pinguis CCMP1416
AF102373 Pavlova pinguis SA19 04
JF714231 Pavlova granifera PLY552*
JF714249 Pavlova gyrans AC28
AF102371 Pavlova gyrans
AF106053 Pavlova lutheri
AF106051 Pavlova gyrans
AF106054 Pavlova gyrans ISR118 09
AF106055 Pavlova gyrans
JF714247 Pavlova pinguis CCAP940/2*
JF714246 Pavlova gyrans CCAP940/1b*
U40922 Pavlova gyrans
JF714248 Pavlova salina CCAP940/3
JF714244 Rebecca salina PLY465*
L34669 Pavlova salina PLY468
AF106059 Pavlova salina
AF102987 Pavlova salina
JF714245 Pavlova sp. AC537
AB183595 Pavlova sp. MBIC10442
AF102372 Exanthemachrysis gayraliae
AF106049 Pavlova sp. J013
AF106048 Exanthemachrysis gayraliae Pav8
AF106050 Exanthemachrysis gayraliae B18X
AF106060 Exanthemachrysis gayraliae YP15
JF714228 Pavlova sp. AC245
JF714227 Pavlova sp. AC35
JF714226 Pavlova sp. AC249
JF714225 Pavlova sp. AC246
JF714224 Pavlova sp. AC37
JF714223 Pavlova sp. AC252
DQ531625 Exanthemachrysis gayraliae AC15*
0.02

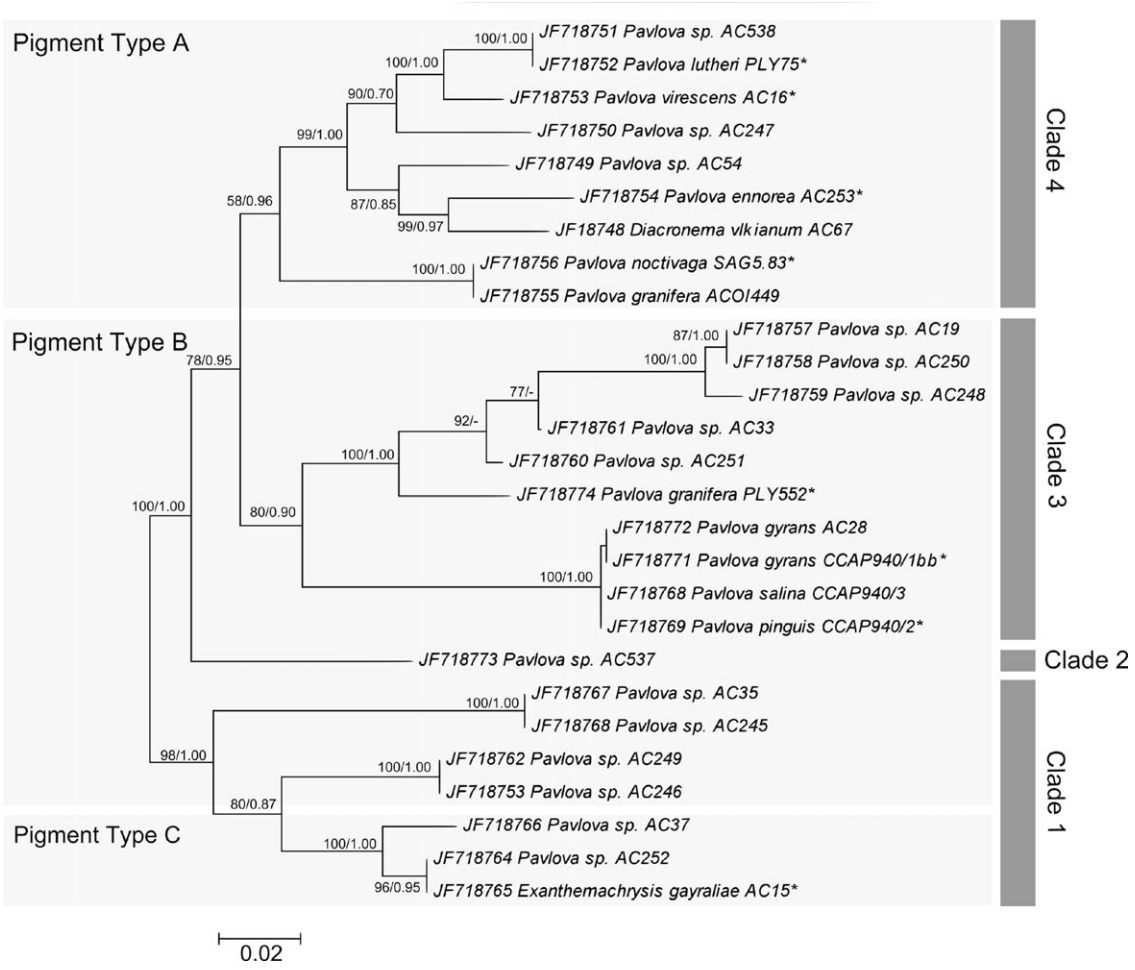

Figure 2. Molecular phylogeny of the Pavlovophyceae inferred from comparison of 28S rDNA sequences. The tree shown resulted from a maximum likelihood analysis using Prymnesiales sequences as an outgroup. Bootstrap percentage values determined for maximum likelihood (>50%) are shown on the left and posterior probability of the bayesian inference on the right. Type strains are marked with an asterisk.

drates in crystalline microfibrillar units forming granules as described by Kiss and Triemer (1988). Crystalline inclusions rich in sulphur and barium and polyphosphate granules have been reported in some members of the class (Fresnel et al. 1979; van der Veer 1976). An eyespot is generally present in association with an invagination of the plasmalemma, but not associated with a flagellar swelling.

Based on a literature survey and our observations, a detailed synthesis of morphological and ultrastructural information for each of the 13 described species is presented in Table 4. A summary of the principal characters for each species is given below.

Exanthemachrysis gayraliae (Fig. 4)

The dominant stage consists of non-motile colonies of slightly ovate cells embedded in multiple layers of mucilage (Fig. 4A and B). The parietal plastid is brownish-green with a bulging pyrenoid that forms a visible protuberance on the cell body (Fig. 4B). The flagella of motile cells do not possess hairs and a haptonema is present (Fig. 4C). A distal string

Figure 1. Molecular phylogeny of the Pavlovophyceae inferred from comparison of 18S rDNA sequences. The tree shown resulted from a maximum likelihood analysis using Prymnesiales sequences as an outgroup. Bootstrap percentage values determined for maximum likelihood (>50%) are shown on the left and posterior probabilities of the Bayesian inference on the right. Type strains are marked with an asterisk.

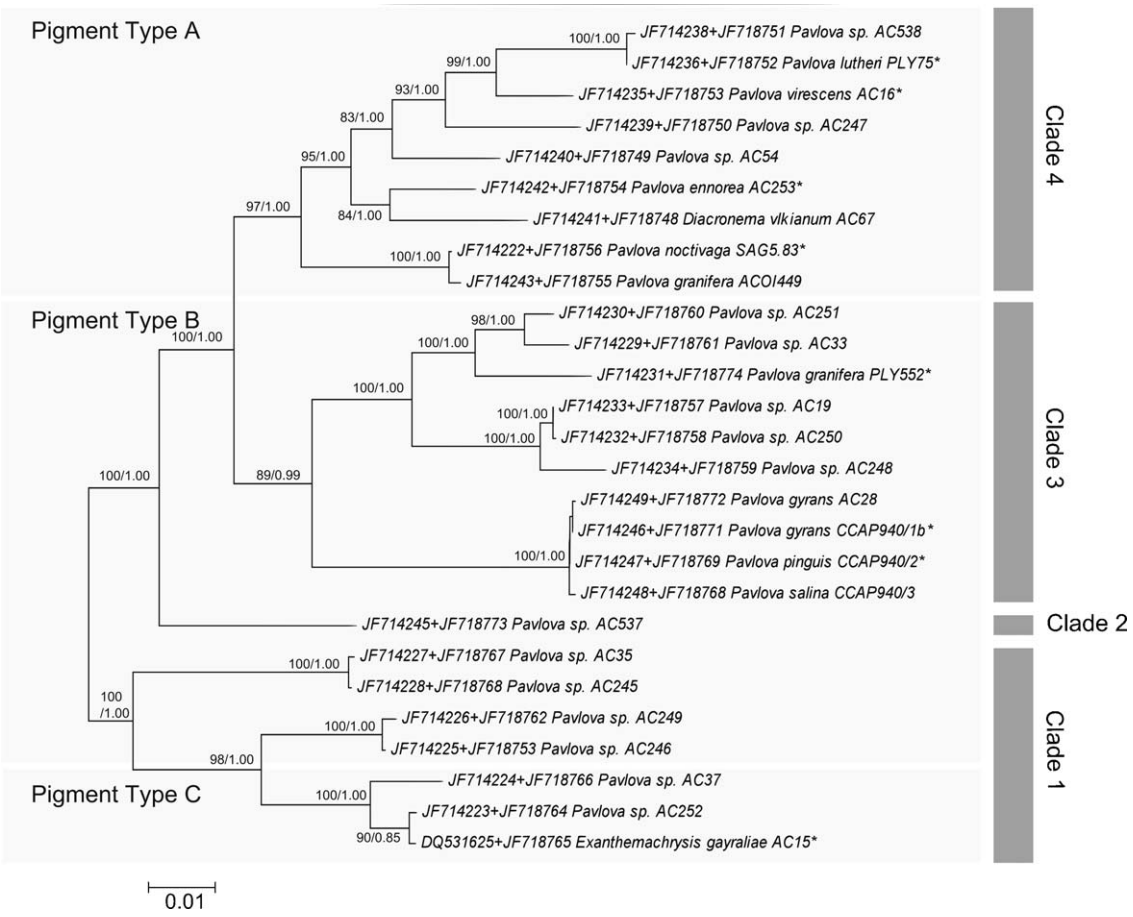

Figure 3. Molecular phylogeny of the Pavlovophyceae inferred from comparison of concatenated 18S rDNA and 28S rDNA sequences. The tree shown resulted from a maximum likelihood analysis using Prymnesiales sequences as an outgroup. Bootstrap percentage values determined for maximum likelihood (>50%) are shown on the left and posterior probabilities of the Bayesian inference on the right. Type strains are marked with an asterisk.

of pearl-like structures is present on the posterior flagellum (Fig. 4C), a feature that has never previously been described. Thylakoid lamellae exhibit a helicoidal arrangement (Fig. 4D) as noticed by van der Veer (1979) for *Rebecca salina* and *R. helicata*, formerly *Pavlova mesolychnon* (van der Veer 1969) and *Pavlova helicata* (van der Veer 1972) respectively. The bulging pyrenoid is delimited from chloroplast stroma by osmiophilic vesicles forming an eyespot (Fig. 4E). The cell body is devoid of knob scales.

Rebecca salina (Fig. 5)

Motile cells are ovate to oblong and slightly metabolic with a golden-green parietal plastid

Table 3. List of primers used in this study.

Primer name	Sequence (5′-3′)	Target gene	References
A18DIR (Forward)	AACCTGGTTGATCCTGCCAGT	SSU rDNA	Medlin et al. 1988
A18 REV (Reverse)	TCCTTCTGCAGGTTCACCTAC	SSU rDNA	Medlin et al. 1988
18SISE (Internal primer)	CTGACACAGGGAGGTAGTGAC	SSU rDNA	Lab use
18S IAS (Internal primer)	TCCTCACTATGTCTGGACCTG	SSU rDNA	Lab use
LEUK2 (Forward)	ACCCGCTGAACTTAAGCATATCACT	LSU rDNA	Liu et al. 2009
EUK_34R (Reverse)	GCATCGCCAGTTCTGCTTACC	LSUrDNA	Liu et al. 2009

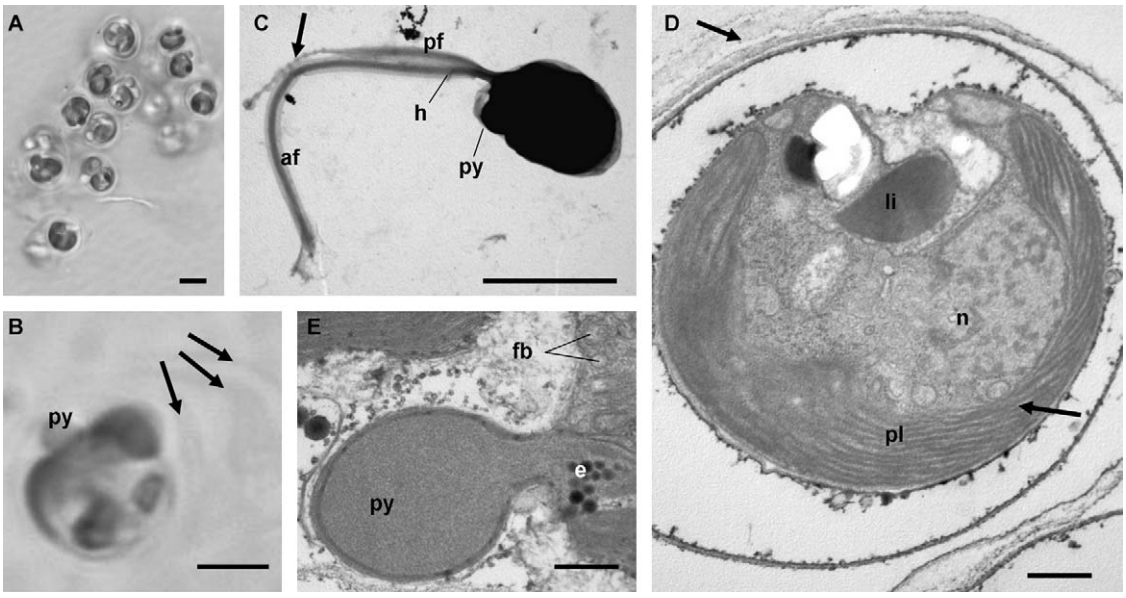

Figure 4. *Exanthemachrysis gayraliae*: **A**. Non-motile colony of cells embedded in mucilage; **B**. Non-motile cell with bulging pyrenoid in stratified mucilage (arrows); **C**. TEM. micrograph of motile cell (negative staining) showing three appendages and a bulging pyrenoid, with a string of pearl-like structures on the posterior flagellum (arrow); **D**. TEM micrograph of motile cell in transversal section showing the nucleus, one parietal plastid with helicoidal arrangement of the thylakoid lamellae (right arrow) and stratified mucilage (left arrow); **E**. TEM micrograph showing section of a pyrenoid and the eyespot; a section of the basal body visible on one side. Scale bar: A, B, C: 5 μm; D, E: 500 nm. Abbrev: af: anterior flagellum, e: eyespot, fb:flagellar base, h: haptomena, li: lipidic droplet, n: nucleus, pf: posterior flagellum, pl: plastid, py: pyrenoid.

(Fig. 5A). The anterior flagellum is visible and bears hairs and knob scales (Fig. 5B). A well-developed haptonema emerges adjacent to the anterior flagellum, sometimes with fine filipodia (Fig. 5B and C). The vestigial posterior flagellum is reduced to the axoneme structure and is covered by small clavate knob scales (Fig. 5D), like the entire cell body external to the plasma membrane (Fig. 5E). A pyrenoid and an eyespot were not observed. One or two plastids are present with a parallel helicoidal arrangement of thylakoid lamellae (Fig. 5F) as in *E. gayraliae*.

Pavlova gyrans (Fig. 6)

The motile phase is dominant and the strongly metabolic cells have a yellow-green parietal plastid with a red-orange eyespot located near the flagellar insertion (Fig. 6A). Filipodia are sometimes observed extending from the cell surface (Fig. 6A, B). The hairy anterior flagellum is covered with knob scales, while the shorter posterior flagellum is naked (Fig. 6B, C and D). The haptonema is often visible (Fig. 6B, C). Smaller body knob scales surround the plasma membrane of the cell body (Fig. 6E). The plastid has parallel thylakoid lamellae, some osmiophilic globules forming an eyespot on the inner face and located near the flagellar pit (Fig. 6F), and a bulging pyrenoid (Fig. 6G).

Pavlova pinguis (Fig. 7)

This species has strongly metabolic motile cells with many filipodia and with a green-yellow parietal plastid (Fig. 7A and B). The three appendages are present: the posterior flagellum is naked (Fig. 7C) whereas the anterior flagellum possesses hairs and knob scales (Fig. 7C and D), with the haptonema inserted between them. Knob scales were not observed on the cell body. A red eyespot is located near the flagellar insertion on the inner face of the plastid (Fig. 7E). Like *P. gyrans*, the plastid has parallel thylakoid lamellae. A bulging pyrenoid is also present (Fig. 7F).

Pavlova granifera (Fig. 8)

Motile cells are strongly metabolic and possess a brown plastid with a red-orange eyespot located near the flagellar insertion (Fig. 8A). The naked posterior flagellum is rigid (Fig. 8A), the anterior flagellum is flexible and covered by hairs and

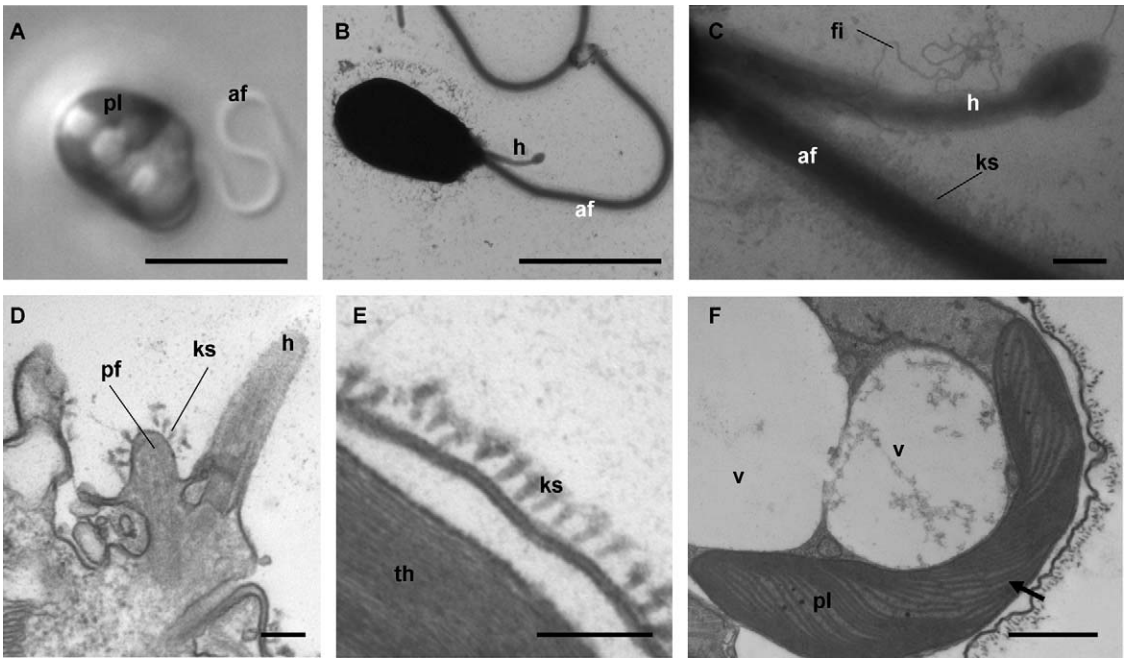

Figure 5. *Rebecca salina*: **A**. Motile cell with conspicuous anterior flagellum; **B**. TEM micrograph of a motile cell (negative staining) with anterior flagellum and haptonema; **C**. Detail of the haptonema and the anterior flagellum bearing knob scales; **D**. TEM micrograph of the haptonema and vestigial posterior flagellum covered with knob scales in longitudinal section; **E**. TEM micrograph of detail of a section showing body knob scales on the plasma membrane; **F**. TEM micrograph of the plastid in transversal section showing the thylakoid arrangement (arrow). Scale: A, B: 5 μm; C, D: 200 nm. Abbrev: af: anterior flagellum, fi: filipodium, h: haptomena, ks: knob scales, pf: posterior flagellum, pl: plastid, th: thylakoids, v: vacuole.

knob scales (Fig. 8A, B and C), and an emergent haptonema is present between the flagella (Fig. 8A). Sections of whole cells demonstrate the high degree of plasticity of cell shape, from compressed to long (Fig. 8D and E). There is also variability in nuclear shape. A pulsate vacuole is present at the centre of the cell, showing a relation with the flagellar pit (Fig. 8D and E). The plastid has parallel thylakoid lamellae, a bulging pyrenoid (Fig. 8D) and an eyespot on the inner face, adjacent to a less osmiophilic zone connected with the flagellar pit (Fig. 8E).

Diacronema vlkianum (Fig. 9)

The dominant stage consists of motile cells that are round to ovate in shape with a slight ventral compression (Fig. 9A, B and C). The brownish-green plastid is parietal and flagella are ventrally inserted near a red eyespot. The anterior flagellum possesses hairs but no knob scales (Fig. 9B); the posterior flagellum is naked. Both flagella exhibit a small distal attenuation and the haptonema is not always visible, but is present (Fig. 9B and C). The eyespot is composed of osmiophilic globules on the external face of the plastid adjacent to the posterior flagellum (Fig. 9C), which has a swelling with a distinctive regular striations (Fig. 9D) as described for the type strain of *D. vlkianum*. The plastid has parallel thylakoid lamellae and does not possess a pyrenoid.

Pavlova ennorea (Fig. 10)

The dominant stage consists of non-motile colonies of slightly compressed cells embedded in mucilage (Fig. 10A). Parietal chloroplasts are golden-brown in colour (Fig. 10A and B). Appendages of motile cells are inserted ventrally (Fig. 10B). The anterior flagellum possesses hairs and is covered by round knob scales (a feature that has not previously been reported for this taxon) and the short posterior flagellum is distally reduced (Fig. 10C and D). Incomplete flagella with knob scales were observed in non-motile cells. Non-motile cells possess peripheral mucilage vesicles and are surrounded by a homogeneous mucilage layer (Fig. 10E). Cells may have two plastids with parallel thylakoid lamellae separated by a large stromatal space (Fig. 10E and F). Flagella are inserted in an invagination near the nucleus in motile cells

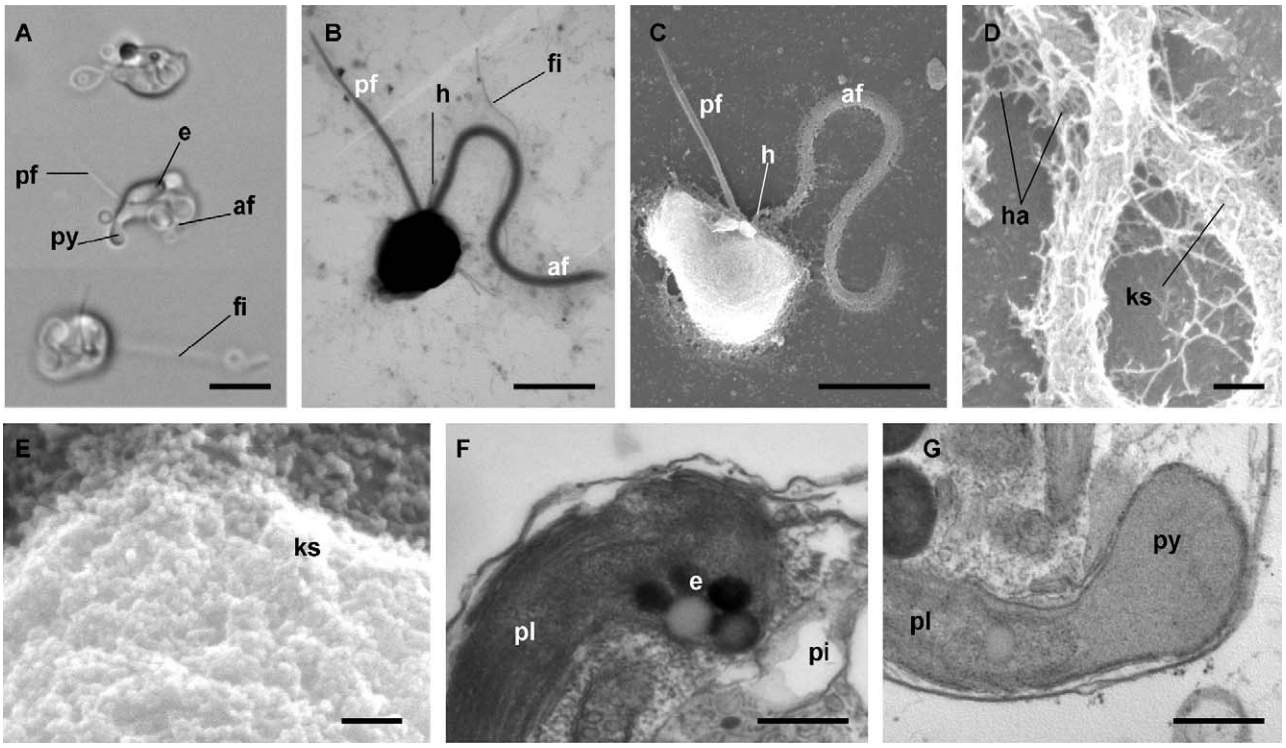

Figure 6. *Pavlova gyrans*: **A**. Highly metabolic motile cells showing 2 flagella, a conspicuous eyespot, a bulging pyrenoid and a filipodium **B**. TEM micrograph (negative staining) of a motile cell with three appendages and a filipodium; **C**. SEM micrograph of a motile cell with three appendages; **D**. SEM micrograph of hairs and knob scales on the anterior flagellum; **E**. SEM micrograph of body knob scales; **F**. TEM micrograph showing section of eyespot; **G**. TEM micrograph of the inner bulging pyrenoid in longitudinal section. Scale bar: A, B, C: 5 μm; D: 200 nm; F, G: 500 nm. Abbrev: af: anterior flagellum, e: eyespot, fi: filipodium, h: haptomena, ha: hair, ks: knob scales, pf: posterior flagellum, pi: flagellar pit, pl: plastid, py: pyrenoid.

(Fig. 10F). This species has no pyrenoid and no eyespot.

Pavlova lutheri (Fig. 11)

The dominant motile cells are mainly round with a yellow-green plastid and a red eyespot (Fig. 11A, B and E). Vacuoles containing a regularly organised crystalline substance were sometimes observed (Fig. 11A). The haptonema is inserted between the hairy anterior flagellum that bears knob scales, unlike the naked posterior flagellum (Fig. 11B and C). The cell body is covered with small knob scales (Fig. 11D). The appendages are inserted near a pit and adjacent to the eyespot which is located on the external face of the plastid (Fig. 11E). Thylakoid lamellae are parallel. A pyrenoid was not observed.

Pavlova noctivaga (Fig. 12)

Motile cells are ovate with a parietal brown-green plastid (Fig. 12A). The anterior flagellum is hairy and is covered by clavate knob scales and the posterior flagellum with a slight distal attenuation is naked (Fig. 12B and C). Cells are sometimes elongate (Fig. 12D). A layer of eyespot globules is present on the external face of the plastid, near the flagellar insertion. A pyrenoid is not present. The plastid presents a simple parallel arrangement of thylakoid lamellae. A pulsate vacuole seems to be connected to the flagellar pit (Fig. 12D).

Pavlova virescens (Fig. 13)

The dominant stage consists of compressed green non-motile cells embedded in mucilage (Fig. 13A) and this stage may form colonies (Fig. 13B). Cells are surrounded by a homogeneous mucilage layer (Fig. 13C). Flagellar bases occur in the ventral depression, the haptonematal base consisting of eight microtubules being inserted between the two flagellar bases (Fig. 13D). Thylakoid lamellae are often stacked, giving a granum-like appearance (Fig. 13E). Absence of thylakoid exvagination indicates that these structures are not grana as in green plants. No stigma and pyrenoid were observed.

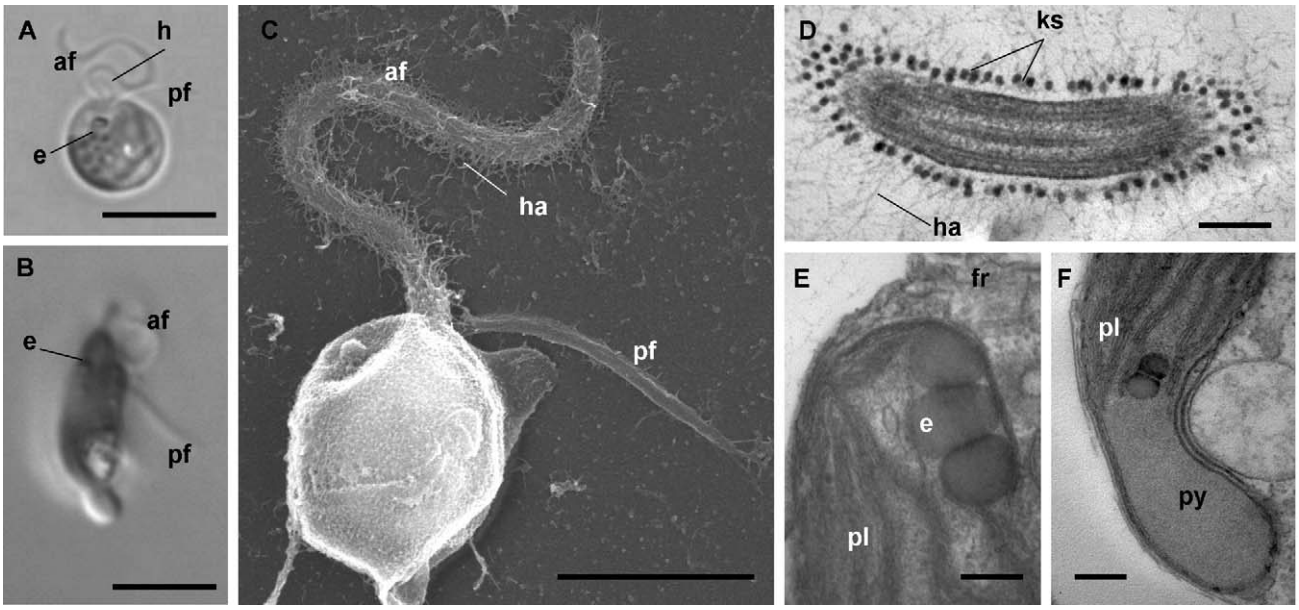

Figure 7. *Pavlova pinguis*: **AB**. Metabolic motile cells (**A**. round **B**. elongated) showing 2 flagella, a conspicious eyespot, a bulging pyrenoid; **C**. SEM micrograph of a round motile cell showing hairy anterior- and glabrous posterior flagella and a filipodium; **D**. TEM micrograph of anterior flagellum with knob scales and hairs in longitudinal section; **E**. TEM micrograph of inner plastid face eyespot at proximity of a flagellar root in longitudinal section; **F**. TEM micrograph of inner bulging pyrenoid in longitudinal section. Scale bar: A, B, C: 5 μm; D, E, F: 200 nm. Abbrev: af: anterior flagellum, e: eyespot, fr: flagellar root, h: haptomena, ha: hair, ks: knob scales, pf: posterior flagellum, pl: plastid, py: pyrenoid.

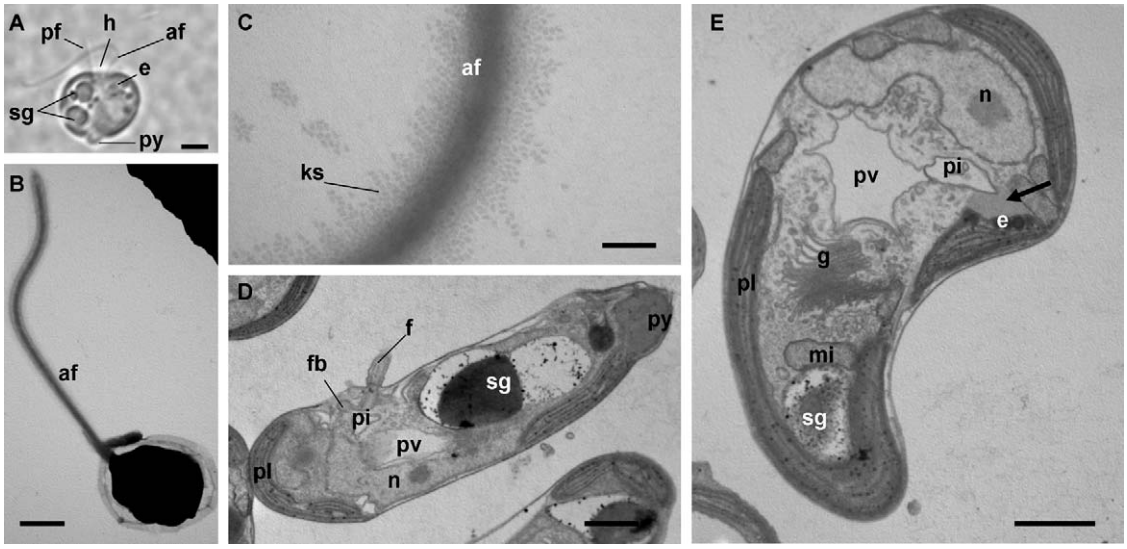

Figure 8. *Pavlova granifera*: **A**. Motile cell showing both flagella, the haptonema, the eyespot, storage (paramylon) granules and a pyrenoid; **B**. TEM micrograph (negative staining) of flagellate cell showing the anterior tomentose flagellum; **C**. TEM (negative staining) micrograph of knob scales covering the anterior flagellum; **DE**. TEM sections of elongate motile cells showing proximity between pulsatile vacuole, flagellar pit and base; **E**. Unidentified contrasted area between flagellar pit and eyespot (arrow). Scale bar: A, B, E: 1 μm; C: 200 nm. Abbrev: af: anterior flagellum, e: eyespot, f: flagellum, fb:flagellar base, g: golgi apparatus, h: haptomena, ks: knob scales, mi: mitochondrion, n: nucleus, pf: posterior flagellum, pi: flagellar pit, pl: plastid, pv: pulsatile vacuole, py: pyrenoid, sg: storage granule.

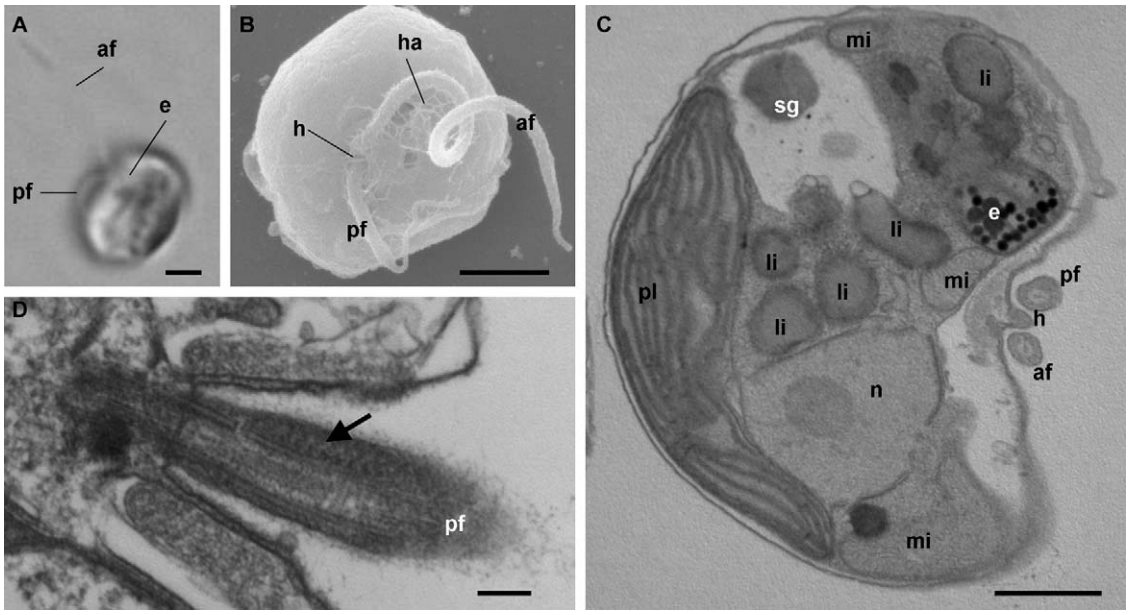

Figure 9. *Diacronema vlkianum*: **A**. Motile cell showing both flagella; **B**. SEM micrograph of the apex of a whole mounted motile cell showing hairy long anterior- and short posterior flagella; **C**. TEM section of a motile cell showing appendage insertion, with a hairy anterior flagellum, a posterior flagellum and the haptonema; **D**. TEM section of posterior flagellum longitudinal, with teeth-like structures (arrow) in the flagellar swelling. Scale bar: A, B, C: 1 μm; D: 200 nm. Abbrev: af: anterior flagellum, e: eyespot, h: haptomena, ha: hair, li: lipidic droplet, mi: mitochondrion, n: nucleus, pf: posterior flagellum, pl: plastid, sg: storage granule.

Pavlova viridis (Fig. 14)

Motile cells are spherical with a green parietal plastid (Fig. 14A). The anterior flagellum and the haptonema emerge from a ventral depression (Fig. 14B and C). The anterior flagellum is covered with knob scales (Fig. 14D). The plastid has parallel thylakoid lamellae, with no eyespot and no pyrenoid (Fig. 14E). The posterior flagellum is reduced to the axoneme structure with only nine single structural microtubules rather than nine triplets (Fig. 14F and G).

Discussion

Based largely on the study of authentic cultures, we present the first full molecular phylogenetic reconstruction of described members of this ancient class of haptophyte algae. In parallel, an ultrastructural re-examination of all described taxa was conducted. This integrative morpho-molecular approach provides the basis for a revision of the taxonomy of the class and insights into the evolutionary ecology of the group.

At the genetic level all described species differ, even in sequences of the conservative 18S rDNA gene, although in some cases, notably *P. pinguis*/*P. gyrans*, differentiation is minor. Sequences from unidentified culture strains and from Genbank indicate the existence of significant microdiversity within the group, part or all of which very probably represents novel species. In this study, four distinct clades were distinguished within the Pavlovophyceae based on the molecular phylogenies. This provides a framework within which to assess the phylogenetic significance of morphological and ultrastructural features.

Clade 1: The only described species in this clade is *Exanthemachrysis gayraliae*. This is the only described member of the Pavlovophyceae that has a ventral bulging pyrenoid and an eyespot formed of osmiophilic vesicles located at the transition between the chloroplast stroma and thylakoids. The complete absence of knob scales is also a distinctive feature, albeit shared with *Diacronema vlkianum* and *Pavlova viridis* that fall in clade 4. The distal string of pearl-like structures on the posterior flagellum is a unique feature that was not reported in the original description of the species. Gayral and Fresnel (1979) transferred *P. ennorea* and *P. noctivaga* to the genus *Exanthemachrysis* based on the fact that motile cells lack flagellar knob scales and non-motile cells apparently lacked external flagellar apparatus. Green (1980) adopted

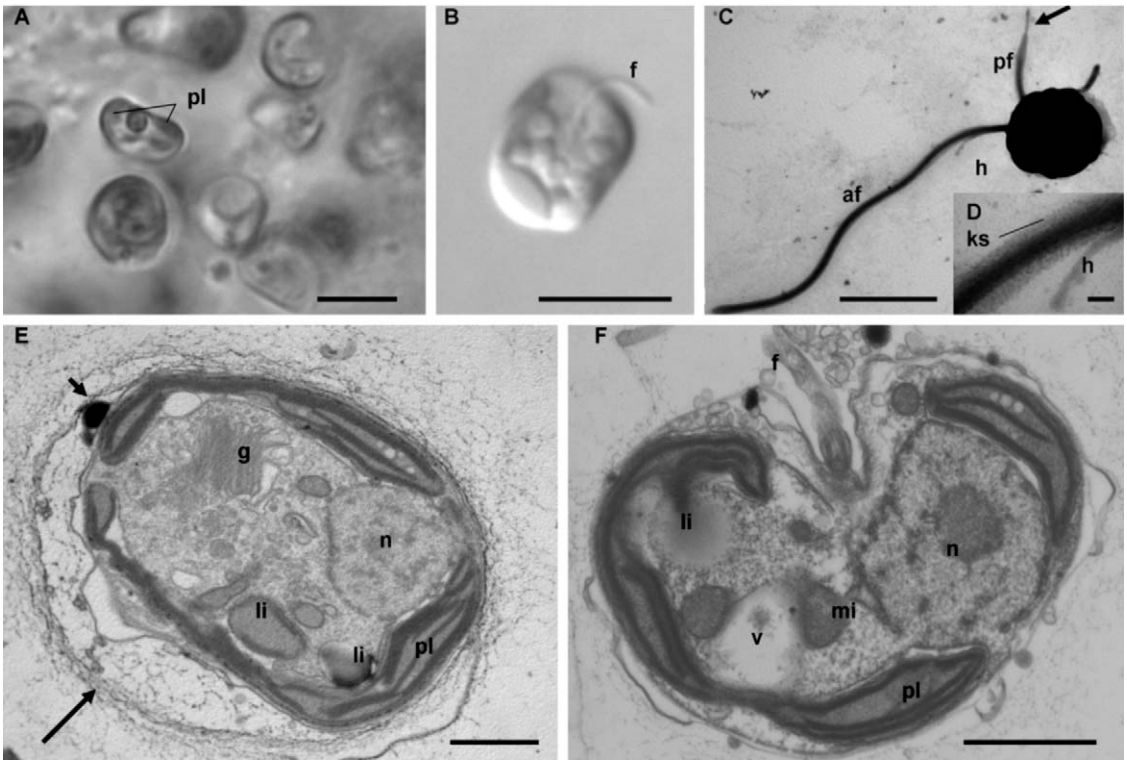

Figure 10. *Pavlova ennorea*: **A**. Colony of non-motile cells; **B**. Apical view of a motile cell with one visible flagellum; **C**. TEM micrograph (negative staining) of a motile cell showing the haptonema near the base of the tomentose anterior flagellum and the shorter attenuated (arrow) posterior flagellum; **D**. Detail of the anterior flagellum covered by knob scales; **E**. TEM section of a non-motile cell surrounded by mucilage (arrows); **F**. TEM section of a motile cell. Scale bar: A, B, C: 5 μm; D: 200 nm; E, F: 1 μm. Abbrev: af: anterior flagellum, f: flagellum, g: Golgi apparatus, h: haptomena, ks: knob scales, li: lipidic droplet, mi: mitochondrion, n: nucleus, pf: posterior flagellum, pl: plastid, py: pyrenoid, v: vacuole.

a more conservative approach of retaining these species in *Pavlova* because the flagellar apparatus of *P. ennorea* was only described as "incomplete" with little detail given by van der Veer and Leewis (1977), whereas Kalina (1975) described and illustrated flagella and haptonema as present in both motile and non-motile cells of *P. noctivaga*. No non-motile cells were present in our culture strain of *P. noctivaga*, but in *P. ennorea* non-motile cells with external flagella covered with knob scales were observed. Our results clearly indicate that *P. ennorea* and *P. noctivaga* do not belong to the genus *Exanthemachrysis*.

Clade 1 includes a number of non-identified strains, most of which are genetically distinct from the type strain, with at least 2 sub-clades likely representing new species (genetic distance equal to or greater than that separating related pairs of described species within the class). All strains we observed from this clade have a dominant non-motile phase. If members of the sub-clades prove to have the same type of pyrenoid and eyespot as *E. gayraliae*, these should logically be classified in the genus *Exanthemachrysis*. It is notable, however, that within this clade only 2 strains closely related to the type strain of *E. gayraliae* share the type C pigment profile (i.e. presence of MV-chl cPAV) with the type species. In Van Lenning et al. (2003), the type strain was the only strain from this clade included in the analysis, hence their conclusion that the presence of MV-chl cPAV is characteristic of the genus and potentially ancestral for the class. Our extended analysis indicates that either (1) the type C pigment profile is not indicative at the genus level, or (2) other sub-clades in clade 1 should be described as a new genus (in fact as at least 2 new genera in order to avoid paraphyly). Ultrastructural examination of other strains in the clade is required to resolve this taxonomic point. The analysis also clearly shows that pigment type C is derived from pigment type B, the latter being the ancestral pigment type for the class.

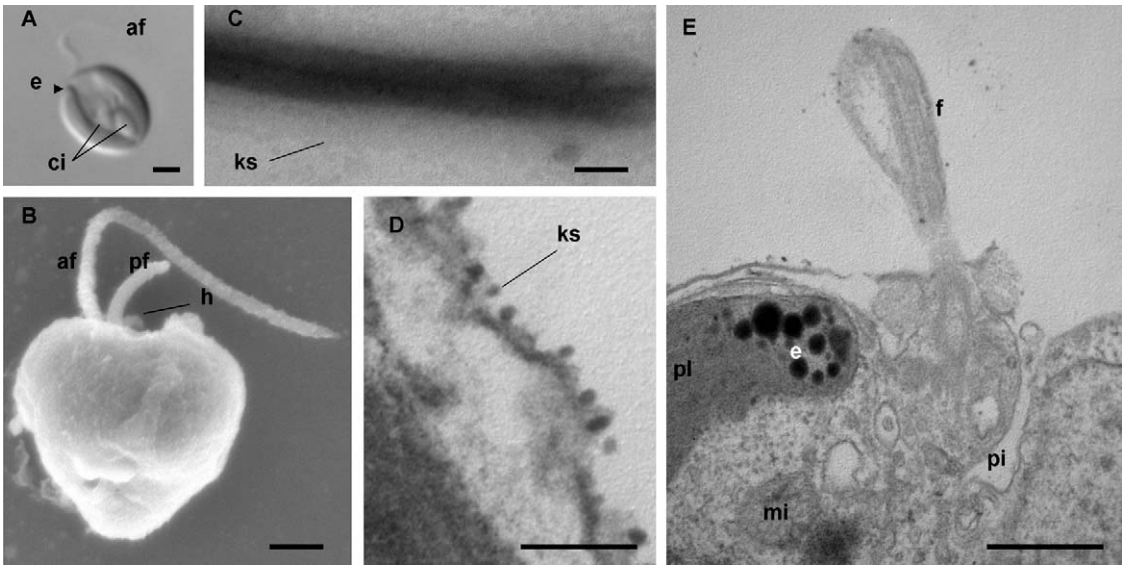

Figure 11. *Pavlova lutheri*: **A**. Motile cell showing the anterior flagellum, crystalline inclusion and the eyespot; **B**. SEM micrograph of a motile cell showing anterior flagellum, posterior flagellum and haptonema; **C**. TEM micrograph (negative staining) of anterior flagellum covered by knob scales; **D**. Details of a section (TEM micrograph) showing body knob scales; **E**. Longitudinal section (TEM Micrograph) showing location of the eyespot and flagellar insertion near a pit. Scale bar: A, B: 1 μm; C: 200 nm; D; 100 nm; E: 500 nm. Abbrev: af: anterior flagellum, ci: crystalline inclusion, e: eyespot, h: haptomena, ks: knob scales, mi: mitochondrion, pf: posterior flagellum, pi: flagellar pit, pl: plastid.

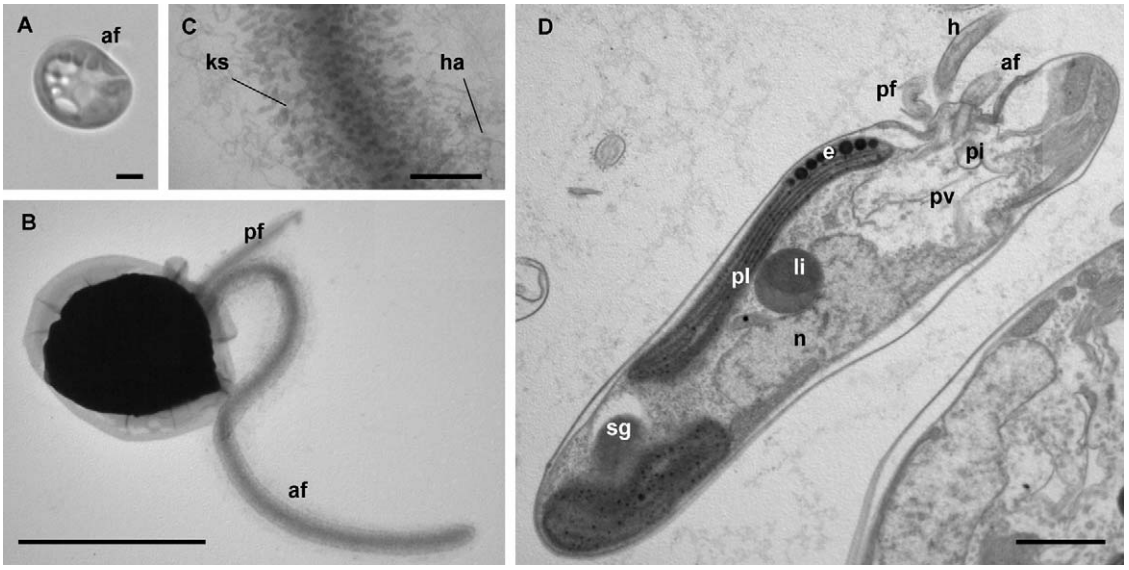

Figure 12. *Pavlova noctivaga*: **A**. Motile cell with an anterior flagellum; **B**. TEM micrograph (negative staining) of a motile cell showing the anterior long tomentose and flexible flagellum and the shorter posterior flagellum; **C**. TEM micrograph of hairy anterior flagellum covered by knob scales (negative staining) **D**. TEM section of a motile cell showing eyespot on the outer face of the plastid and a pulsatile vacuole near the flagellar pit at the base of flagellar apparatus. Scale bar: A: 1 μm, B: 5 μm; C: 200 nm; D: 1 μm. Abbrev: af: anterior flagellum, e: eyespot, h: haptomena, ha: hair, ks: knob scales, li: lipidic droplet, n: nucleus, pf: posterior flagellum, pi: flagellar pit, pl: plastid, pv: pulsatile vacuole, sg: storage granule.

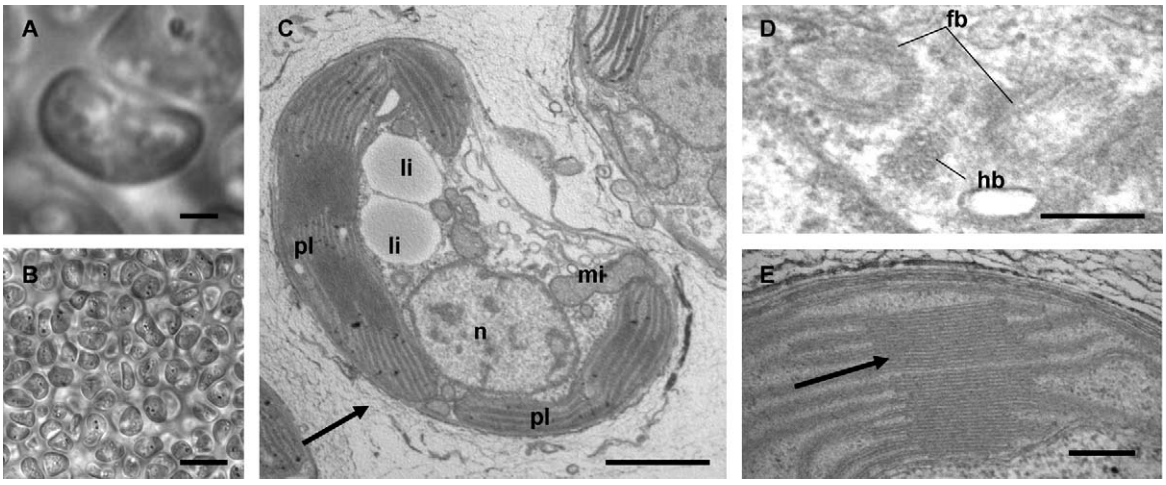

Figure 13. *Pavlova virescens*: **AB**. Non-motile cells in colonies; **C**. TEM section of a motile cell surrounded by mucilage (arrow) showing two plastids, lipidic droplets and mitochondrium; **D**. TEM micrograph of flagellar and haptonematal bases; **E**. TEM section of plastid with granum-like thylakoid arrangement (arrow). Scale bar: A: 1 μm; B: 10 μm; C: 1 μm; D, E: 200 nm. Abbrev: fb:flagellar base, h: haptomena, hb: haptonema base, li: lipidic droplet, mi: mitochondrion: nucleus, pl: plastid.

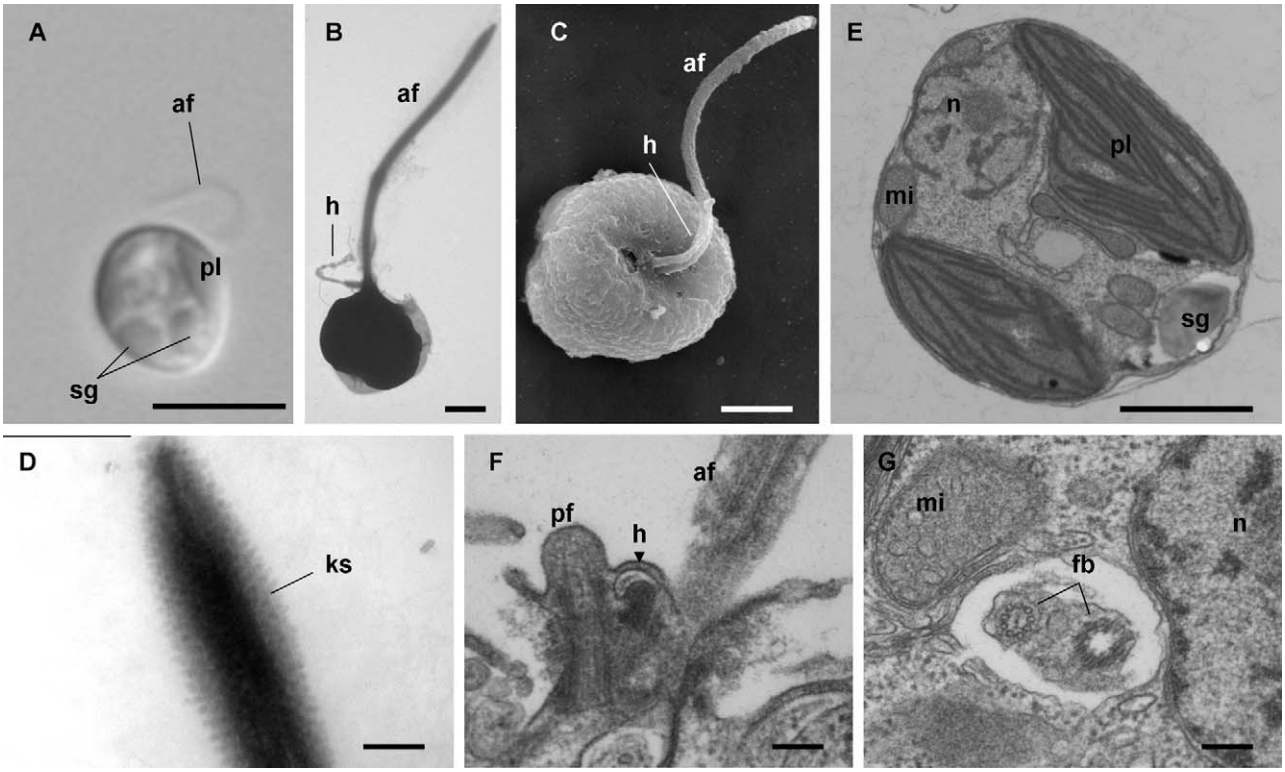

Figure 14. *Pavlova viridis*. **A**. Motile cell with anterior flagellum visible; **B**. TEM micrograph of motile cell with anterior flagellum and haptonema (negative staining); **C**. SEM micrograph of apical view of a motile cell with anterior flagellum and haptonema; **D**. TEM micrograph of anterior flagellum covered by knob scales (negative staining); **E**. TEM section of a motile cell; **F**. TEM micrograph of haptonema and vestigial posterior flagellum in longitudinal section; **G**. TEM micrograph of haptonema and vestigial posterior flagellum in transversal section. Scale bar: A: 5 μm; B, C: 1 μm; D: 200 nm; E, 1 μm; F, G: 200 nm. Abbrev.: af: anterior flagellum, fb:flagellar base, h: haptomena, ks: knob scales, mi: mitochondrion, n: nucleus, pf: posterior flagellum, pi: flagellar pit, pl: plastid, pv: pulsatile vacuole, py: pyrenoid, sg: storage granule.

Clade 2: This clade is composed of five sequences and includes that of the type strain of the genus *Rebecca*, *R. salina* PLY465. The four other sequences, one from an undescribed strain (AC537) and three Genbank sequences labelled as *Rebecca salina* (or *Pavlova salina*) are all different. Based on a combination of ultrastructural features and molecular phylogeny, *P. salina* was transferred to the new genus *Rebecca* by Edvardsen et al. (2000). According to Edvardsen et al. (2000) a unique feature of this genus, which also includes *R. helicata*, is the vestigial nature of the posterior flagellum. However, this feature is also observed in *P. viridis* (which falls into clade 4). Another feature considered distinctive of *Rebecca* was the lack of an eyespot, but *P. ennorea* and *P. viridis* from clade 4 also lack an eyespot. Unlike *P. viridis*, *Rebecca* possesses knob scales, a feature that remains phylogenetically relevant for this clade. The unusual intra-plastidial structure consisting of thylakoid lamellae separated by large inter-lamellar spaces reported in both *R. salina* and *R. helicata* has been classed as a pyrenoid (Green 1976, van der Veer 1979), but there is doubt as to the exact nature of this structure. Green mentioned that *R. salina* (as *P. salina*) has 'no obvious pyrenoid' (Edvardsen et al. 2000), and likewise we did not observe a structure that can be considered to be a pyrenoid in *R. salina*. The absence of a pyrenoid is a feature shared with clade 4 and notably with *P. ennorea* that possesses similar intra-lamellar spaces between thylakoid lamellae. To our knowledge, the type strain of *R. helicata* no longer exists and it will therefore be difficult to prove that it belongs to *Rebecca*, although further study of strain AC537 and other cultures in this clade may help.

It should be noted that Edvardsen et al. (2000) based their taxonomic revision (creation of the genus *Rebecca*) on the sequence of the culture strain PLY468 (labelled as *Pavlova aff. salina*) that is not the type strain of *R. salina*. The 18S rDNA sequence of the type strain (PLY465) studied here is not identical to that of PLY468, the latter is, therefore, likely to be a different species. However, the proximity of these two strains within clade 2 in our molecular phylogeny indicates that the revision proposed by Edvardsen et al. (2000) is indeed warranted. Comparison of ribosomal gene sequences clearly separates *Rebecca* from other members of the Pavlovales, but pigment profiles do not separate the *Rebecca* clade from clade 3 and most of clade 1, and there is no single unique ultrastructural feature that distinguishes the clade. The *Rebecca* clade (as represented by the type strain of *R. salina*) does, however, exhibit a unique combination of features, namely vestigial posterior flagellum, lack of eyespot, presence of knob scales, lack of pyrenoid and pigment type B.

Clade 3: This clade includes sequences of the type strains of *P. granifera*, *P. gyrans* and *P. pinguis*. Clade 3 is composed of two clear sub-clades.

Clade 3.1: This sub-clade contains the type strains of both *P. pinguis* (CCAP940/2) and *P. gyrans* (CCAP940/1b) that have identical 18S rDNA sequences (with 4 bp difference in ITS sequences; data not shown) and no difference in 28S rDNA sequences. Similarity in flagellar structure and in the arrangement of the pit, eyespot, chloroplast and pyrenoid between *P. pinguis* and *P. gyrans* prove clear affinities between them (Green 1980). Minor ultrastructural differences noticed by Green (1980) included less osmiophilic droplets in *P. pinguis* and the presence of hairs on the short flagellum of *P. gyrans* (that of *P. pinguis* being naked). We did not observe an obvious difference in the quantity of osmiophilic droplets and we did not observe hairs on the short flagellum of either species (or any other pavlovophycean taxon). The presence/absence of knob scales is the only differential feature between the two species noted by Green (1980) that was confirmed in our study. In the context of the extreme genetic similarity between the two type strains, the significance of this morphological difference is not clear. The presence/absence of knob scales and very minor genetic difference could be the result of a recent speciation event, but it is also possible that presence/absence of knob scales is a phenotypic difference within a single species (the name *P. gyrans* having priority). In this latter context, it is noteworthy that differences in scale morphology characterise haplo-diploid life cycle stages in the Prymnesiophyceae (Billard 1994; Houdan et al. 2004). In most known cases in the Prymnesiophyceae, the two life cycle stages both possess body (plate-type) scales with different ornamentation between the stages, but there are examples (most notably the coccolithophore *Emiliania huxleyi*) where one phase possesses scales and the other phase does not (Green et al. 1996; Houdan et al. 2004; Klaveness, 1972). Digenetic and/or dimorphic life cycles have never been reported in the Pavlovophyceae, but the possibility that *P. gyrans* and *P. pinguis* could be different forms within a common life cycle should be considered.

Pavlova gyrans, described by Butcher (1952), is the type species of the genus, and this subclade thus retains the name *Pavlova*. A number of sequences from other culture strains (from our analysis and from Genbank) are identical or very similar to those of *P. gyrans*/*P. pinguis* and together

these form a definite sub-clade, potentially representing recent radiation within a *P. gyrans* species complex.

A problem was encountered during examination of the strain CCAP940/3 that was labelled as being equivalent to PLY465, the type strain of *Rebecca salina*, but which exhibited an 18S rDNA sequence and morphological characters with close affinity to *Pavlova pinguis*. The original type strain, PLY465, which we confirmed to have the ultrastructural characters of *R. salina*, is in the Plymouth Culture Collection as *Pavlova salina*.

Clade 3.2: There is a clear genetic distinction between this second sub-clade and sub-clade 3.1. The type strain of *Pavlova granifera* (PLY552), a freshwater species with ultrastructural characters similar to *P. pinguis* and *P. gyrans*, is part of this sub-clade. The brackish strain AC33 has a sequence close to that of *P. granifera* and the ultrastructure of both strains is similar. *Pavlova granifera* does not possess knob scales (like *P. pinguis*), but there are no other obvious ultrastructural differences between *P. granifera* and *P. gyrans/P. pinguis* except the presence of a pulsatile vacuole in *P. granifera*, that is likely to be the consequence of being cultured in a freshwater medium (cf. the conclusion of Green and Hibberd (1977) for *Diacronema*). *Pavlova granifera* was described (as *Chrysocapsa granifera*) before *P. gyrans* (and *P. pinguis*), but only by light microscopy (Mack 1954). Green (1973) observed the type strain of *P. granifera* using electron microscopy only after the descriptions of *P. gyrans* and *P. pinguis* and it is clearly possible that strains of the latter two species could have been classified as *P. granifera* had this chronology been different. However, we consider that *P. granifera* and *P. gyrans/P. pinguis* should be maintained as separate species due to the genetic difference between them, and in this context habitat (freshwater/brackish vs marine) could have resulted in speciation between the sub-clades. This sub-clade also contains Genbank sequences mostly labelled as *P. pinguis*, as well as AC19 (a marine strain) that had also been identified as *P. pinguis* by TEM. We propose maintenance of this sub-clade in the genus *Pavlova* in view of the evident morphological and ultrastructural affinity with clade 3.1. It seems clear, however, that this genus contains a number of cryptic entities.

Clade 4: This clade contains the type strains of *P. noctivaga* (SAG5.83), *P. lutheri* (PLY75), *P. ennorea* (AC253), *P. virescens* (AC16) and *P. viridis* (ASIO3012). The type strain of *D. vlkianum* is no longer available, but strain AC67 exhibits ultrastructural characters identical to the original description and thus is taken as being representative of *D. vlkianum*. This clade is distinguished by occurrence of pigment type A (lack of chl cPAV) in all examined strains. In terms of ultrastructure, however, this is the most diverse clade. Each species exhibits distinctive ultrastructural characters, but unifying features are the absence of a pyrenoid, the presence of scales (except *D. vlkianum*), the presence of an inconspicuous eyespot on the outer face of the chloroplast (except *P. viridis* and *P. ennorea*) and 'normal' anisokont flagella (except *P. viridis* and *D. vlkianum*).

Diacronema vlkianum is distinguished by the unique structure of the posterior flagellum, which has a proximal part swollen on the side adjacent to the cell, and the ventral position of the flagellar insertion (Green and Hibberd 1977). The absence of scales in *D. vlkianum* is also unique within this clade. *D. vlkianum* was basal to this clade in the phylogeny of Van Lenning et al. (2003), but falls within the clade in our extended phylogenies based on both 18S and 28S rDNA sequences. This provides a strong indication that these characters related to flagellar structure and positioning and lack of scales are not taxonomically relevant above the species level and that maintenance of this species in a separate genus from other members of this clade is not justified.

Four possibilities were proposed by Van Lenning et al. (2003) for the taxonomy of this clade: 1) *Diacronema vlkianum* could be transferred to *Pavlova* if certain morphological (presence/absence and structure of pyrenoid and eyespot) and pigment (presence/absence of DV-chl cPAV) features are not considered taxonomically relevant; 2) *Pavlova lutheri* and *P virescens* (and potentially *P. calceolata* and *P. noctivaga*) may be transferred to an emended genus *Diacronema* if the latter morphological and pigment groupings are considered relevant and the *D. vlkianum* flagellar morphology does not prove to be significant; 3) a new genus may be created to contain *P. lutheri* and *P virescens* (and potentially *P. calceolata* and *P. noctivaga*) if all of these features are considered relevant; and 4) the current taxonomy can be retained, leaving *Pavlova* as a paraphyletic, but non-polyphyletic, genus. Based on the clear genetic differentiation of this clade from clade 3, together with the unifying features of the lack of a pyrenoid and lack of chl cPAV, we consider that option 2 is the most rational and we therefore propose the transfer of all species in this clade to an emended genus *Diacronema*. *Pavlova calceolata* was not studied here since the type strain no longer exists, but

published ultrastructural characters clearly show that it belongs to this clade and therefore that it should also be transferred to *Diacronema*.

Evolutionary Ecology

According to the molecular clock estimation of Liu et al. (2010) (and assuming that the evolutionary rate of the 28S rRNA gene is comparable across haptophytes), the divergences between the 4 extant clades of the Pavlovophyceae are very ancient. The *Exanthemachrysis* clade is estimated to have diverged around the time of the Permian/Triassic boundary ca. 250 Mya, the *Rebecca* clade diverged in the Jurassic ca. 170 Mya and the *Pavlova* and *Diacronema* clades diverged in the Cretaceous ca. 100 Mya. This provides strong additional support for taxonomic separation into 4 discrete genera following the delineation into clades presented here and indicates that the existing genera have traversed one or more major global extinction events. Medlin et al. (2008) suggested that the adaptation of certain non-calcifying prymnesiophytes to eutrophic coastal environments and their ability to switch modes of nutrition from autotrophy to mixotrophy are possible explanations for survival across the K/T boundary. Pavlovophytes are known mainly from culture strains isolated from near-shore coastal environments and the described species clearly thrive in rich culture media reminiscent of eutrophic environments. There is a general conception that all extant members of the Pavlovophyceae rely exclusively on photosynthesis as a source of nutrition (e.g. Cavalier-Smith 2002; de Vargas et al. 2007), but to our knowledge there have been no specific attempts to determine whether members of this class are capable of phagotrophy (and hence mixotrophy). Many chromalveolate algae with comparable body plans are capable of bacterivory and this may yet be proved to be the case in the Pavlovophyceae.

Given the ancientness of pavlovophyte lineages and their apparent robustness to major global change events, it is perhaps surprising that diversity within this group is apparently relatively limited (13 described species vs ca. 400 in the Prymesiophyceae). We provide molecular genetic evidence that the group is more diverse than previously thought, but diversity remains low compared to that known in the Prymnesiophyceae (particularly in light of the recent results of Liu et al. 2009) and to that of most other microalgal classes. This is probably in part due to the fact that pavlovophytes are relatively difficult to identify in natural samples using classical microscopy techniques and we therefore predict that future culture-based studies and particularly culture-independent metagenomic analyses will reveal more new diversity within this class, as pointed out by Shi et al. (2009). If, however, diversity in this group does prove to remain low, the question of why this should be the case links into the debate on the origins of the class: are the Pavlovophyceae living fossil relics of simple ancestral haptophytes or are they derived forms highly specialised for a particular type of ecological niche?

Certain predictions can be made as to the likely nature of the cenancestor of the known Pavlovophyceae based on the topology of our molecular phylogenetic reconstruction. It was probably an estuarine/marine organism with anisokont, subapically inserted flagella (with non-tubular hairs on the long anterior flagellum), a non-coiling haptonema, simple flagellar roots (associated only with the base of the mature short posterior flagellum), a primitive eyespot and a simple pigment profile with MV chl cPAV. It is not clear whether this ancestral pavlovophyte would have possessed knob scales (due to absence in the *Exanthemachrysis* clade) or a pyrenoid (absence in the *Rebecca* and *Diacronema* clades). This picture for the ancestral pavlovophyte differs rather radically from the likely nature of the ancestral prymnesiophyte, which is likely to have possessed isokont, smooth, apically inserted flagella and a forward pointing, non-coiling haptonema with several microtubules in the emergent part, relatively complex flagellar roots, plate scales, and a pyrenoid (de Vargas et al. 2007; Edvardsen et al. 2000). The pigment profile of early prymnesiophytes is likely to have been the same as that of pavlovophyte pigment type A, meaning that chl cPAV evolved early in the Pavlovophyceae lineage after divergence from the Prymnesiophyceae. Stigmata have never been observed in the Prymnesiophyceae and were presumably absent in the cenancestor of this group. Cavalier-Smith (1994) proposed that it is likely that anisokonty with asymmetrical cell shape is the ancestral state for all Haptophyta due to the predominance of this body plan in chromist algae. However, the same author (Cavalier-Smith 2002) later considered that the loss of tubular flagellar hairs in haptophytes was essential for the evolution of a functionally correlated forward-pointing haptonema and homodynamic isokont cilia and that predatory prymnesiophytes retain this condition, whereas the purely photosynthetic Pavlovophyceae became secondarily anisokont, moving the kinetid to the cell apex and therefore losing the roots associated with the anterior flagellum.

Although it has not been satisfactorily proved that pavlovophytes are purely photosynthetic, and despite the fact that the asymmetrical body plan with anisokont flagella is widespread in chromalveolate algae, it does seem that a number of the apparently simple characters of the pavlovophytes are derived. These include the reduction in the number of microtubules in the emergent part of the haptonema (most prymnesiophytes have at least 6 microtubules in the emergent part of the haptonema, when present), the loss of roots associated with the anterior flagellum (most chromalveolates have microtubular roots associated with both flagellar bases), the presence of simple non-tubular hairs on the anterior flagellum (these not being structurally comparable with bi- or tripartite mastigonemes in heterokonts), and the eyespot (the pavlovophyte stigmata do not have obvious homologies within the chromalveolates and in fact most closely resemble certain structures present in the green lineage). The fact that there is not a very high level of morphological diversity amongst known pavlovophytes despite divergence times of as much as a quarter of a billion years could be interpreted as indicating that the lineage has adopted a structure that is particularly well suited for a specific niche (near-shore coastal environments), but that this structure is fundamentally not very plastic in evolutionary terms. The existence of two phylogenetically distant extant freshwater pavlovophyte species, together with the occurrence of euryhaline species like *D. vlkianum*, indicates multiple invasions of freshwater, but there is little evidence that members of this class have managed to become established in more oligotrophic ecosystems. It will be particularly interesting to see from future metagenomic studies whether pavlovophytes are present (and diverse) in open ocean environments. Shi et al. (2009) provide the first evidence that this may be the case.

Concluding Remarks

The combination of morphological, molecular genetic and biochemical analyses employed here is shown to be a powerful tool for phylogenetic reconstructions and verification of the taxonomic validity of species described using classical techniques only. In this context, the accuracy of classical techniques for distinguishing species is noteworthy. Our analysis confirms that most of the described species are discrete taxonomic entities, with one possible cryptic exception involving *P. gyrans* and *P. pinguis*. The existence of type strains as reference material is invaluable for this type of revaluation. Access to type strains allowed verification of certain contentious points, discovery of new features in some species, and detection of the accidental mislabelling of a supposed type strain. This latter experience highlights the importance of independently verifying the identity of strains obtained from culture collections, a fact that most service collections are aware of and are addressing notably through the implementation of genetic barcoding of culture holdings.

We have highlighted the need for complementary studies on known pavlovophyte species, notably in terms of nutritional capacities and life cycle strategy. The class Pavlovophyceae contains a significant amount of undescribed diversity already in culture. The taxonomic scheme proposed in this study will provide a framework for describing this new diversity and for interpreting imminent environmental gene sequencing efforts.

Taxonomic Summary

REVISED DIAGNOSES OF DIACRONEMA Prauser emend. Bendif et Véron

Motile cells with two unequal flagella and a short haptonema. Longer anterior flagellum with fine non-tubular hairs and with or without of minute dense bodies; posterior flagellum sometimes with a basal swelling and vestigial. Occasionally dense bodies on cell surface. A pit or canal penetrating the cell near the long anterior flagellum. Chloroplast single or double without a pyrenoid, sometimes with an eyespot located on the external face of the plastid. Non-motile cells with or without incomplete appendages.

Mobiles cellulae duobus inaequalibus flagellis et brevi haptonema instructae. Longum flagellum anterius cum tenuibus non tubularibus pilis atque cum aut sine minutis densisque corporibus, posterius autem flagellum interdum vestigiale et interdum cum basali tumore. Aliquando densa corpora in summa cellula. Fovea vel canalis penetrat cellulam prope longum flagellum. Chloroplastus unicus vel geminus sine pyrenoide, interdum cum stigmate in externa facie plastidi sito. Immobiles cellulae imperfecto appendice praesente aut deficiente.

TYPE SPECIES: *Diacronema vlkianum* Prauser

BASIONYM: *Diacronema vlkianum* Prauser 1958 Arch Protistenkd 103: 117-128

Diacronema ennorea (Veer et Leewis) Bendif et Véron comb. nov.

BASIONYM: *Pavlova ennorea* Veer et Leewis 1977 Acta Bot Neerl 26: 159-176

Synonym: *Exanthemachrysis ennorea* (Veer et Leewis) Gayral et Fresnel 1979 Protistologica XV: 271-282

REVISED DIAGNOSIS of *Diacronema ennorea* Veer et Leewis 1977 emend. Bendif et Véron

Sedentary cells forming non-motile colonies, slightly compressed or often flattened if touching each other. Homogeneous mucilage excretion with osmiophilic muciferous vesicles. Plastid single, yellow green, without eyespot or pyrenoid and thylakoid lamellae parallel with large stromatal space. Motile cells elongate with two unequal flagella and a haptonema. Anterior flagellum with fine hairs and circular knob scales. Flagellar insertion in a slight ventral depression. Absence of body scales.

Sedentariae cellulae colonias immobiles formantes, leviter compressae vel saepius complanatae, si inter se contingentes. Homogenae mucilagini excretio cum muciferis vesiculis homogeneis. Unicus chloroplastus, flavovirens, nec stigmate nec pyrenoide instructus, ac thylacoides et parallelae lamellae cum magno stromatico spatio. Mobiles cellulae elongatae duobus flagellis inaequalibus et haptonema instructae. Anterius flagellum cum tenuibus pilis ac punctiformibus circularibusque squamis. Insertio flagellorum in levi depressione ventrali. Absentia squamarum cellularium.

DIAGNOSTIC FIGURE: Fig. 10

Diacronema lutheri (Droop) Bendif et Véron comb. nov.

BASIONYM: *Monochrysis lutheri* Droop 1953 Acta Bot Fenn 51: 3-52

SYNONYM: *Pavlova lutheri* (Droop) Green 1975 J mar biol Ass U.K. 55: 785-793

Diacronema noctivaga (Kalina) Bendif et Véron comb. nov.

BASIONYM: *Corcontochrysis noctivaga* Kalina 1970 Preslia 42: 297-302

SYNONYMS: *Pavlova noctivaga* (Kalina) Veer et Leewis 1977 Acta Bot Neerl 26: 159-176, Green 1980 Br Phycol J 15: 151-191, *Exanthemachrysis noctivaga* (Kalina) Gayral et Fresnel 1979 Protistologica XV: 271-282,

REVISED DIAGNOSIS of *Diacronema noctivaga* Kalina 1970 emend. Bendif et Véron

Free living cells mainly ovate or elongate with appendages inserted near a red eyespot. Three remarkably unequal appendages with a hairy anterior flagellum covered by knob scales and a naked posterior flagellum with slight distal attenuation. Absence of body scales. Brown plastid with a layer of eyespot globules present on the external face near the appendage insertion, without a pyrenoid. A pulsate vacuole connected to the flagellar pit. Occurrence of non-motiles colonies with stratified mucilage.

Cellulae solutae saepissime ovatae vel elongatae cum appendicibus prope rubro stigmate insertis. Tres appendices notabiliter inaequales, ex quibus anterius flagellum pilosum punctiformibus squamis coopertum et posterius flagellum nudum cum levi attenuatione distali. Absentia squamarum cellularium. Spadiceus chloroplastus, globulis stigmaticis adlineatis in externa facie prope insertionem appendicum praesentibus, sine pyrenoide. Pulsans vacuola puteo flagillari iuncta. Praesentia coloniarum immobilium cum mucilagine stratificata.

DIAGNOSTIC FIGURE: Fig. 12

Diacronema virescens (Billard) Bendif et Véron, comb. nov.

BASIONYM: *Pavlova virescens* Billard 1976 Soc Phycol de France Bull 21: 18-27

SYNONYM: *Exanthemachrysis virescens* (Billard) Gayral et Fresnel 1979 Protistologica XV: 271-282

Diacronema viridis (Tseng, Chen et Zhang) Bendif et Véron, comb. nov.

BASIONYM: *Pavlova viridis* Tseng, Chen et Zhang 1992 Chin J Oceanol Limnol 10: 23-28

Revised diagnosis of the genus *Pavlova* Butcher ex Green, emended Bendif et Véron

Motile cells, free swimming, strongly metabolic, with two unequal flagella and a short haptonema. Longer anterior flagellum with fine non tubular hairs and minute dense bodies, present or absent on the cell body. A pit or canal penetrating the cell near the long anterior flagellum. Plastid with posterior bulging pyrenoid and eyespot conspicuous on inner surface near the flagellar pit. Non-motile cells with incomplete appendages.

Mobiles cellulae, solute natantes, vehementer metabolicae, duobus inaequalibus flagellis et brevi haptonema instructae. Longum flagellum anterius cum tenuibus non tubularibus pilis ac minutis densisque corporibus, praesentibus aut absentibus in cellulari corpore. Fovea vel canalis cellulam prope longum flagellum anterius penetrans. Chloroplastus cum protuberante pyrenoide et visibili stigmate in interna facie prope puteum flagellarem. Immobiles cellulae imperfectis appendicibus praesentibus.

TYPE SPECIES: *Pavlova gyrans* Butcher

BASIONYM: *Pavlova gyrans* Butcher 1952 J mar biol Ass U.K. 31: 175-191

REVISED DIAGNOSIS of *Exanthemachrysis gayraliae* Lepailleur 1970, emend. Bendif et Véron

Dominant stage of non-motile cells slightly ovate, embedded in a multilayered mucilage. Brownish-green parietal plastid with a bulging pyrenoid forming a protuberance on the cell body. Motile metabolic cells with three naked appendages and a distal string of pearl-like structures on the posterior flagellum attenuation. Bulging pyrenoid delimited from chloroplast stroma by globules forming an eyespot near the insertion of the appendages.

Status dominans immobilium et leviter ovotarum cellularum pluristratificata mucilagine stipatarum. Parietalis chloroplastus olivaceus cum protuberante pyrenoide formante protubertionem in summo cellulari corpore. Mobiles et metabolicae cellulae cum tribus appendicibus et distali catena, margaritis similis structurae, in attenuatione posterioris flagelli sita. Protuberans pyrenoides globulis stigma prope insertionem appendicum formantibus a stromate chloroplasti delimitatus.

DIAGNOSTIC FIGURE: Fig. 4

Methods

Algal cultures: Twenty-nine strains of *Pavlovophyceae* were used in this study, including 10 authentic cultures (Table 2). Cultures were obtained from either Algobank-Caen or other

Table 4. Comparison of principal characters of the Pavlovales (adapted from Green 1980).

Phylogenetic clade		1	2		3					4				
Pigment profile		C	B?	B?	B	B	B	A?	A	A	A	A	A	A
Genus		Exanthemachrysis	Rebecca		Pavlova					Diacronema				
Species		gayraliae	helicata	salina	granifera	gyrans	pinguis	calceolata	ennorea	lutheri	noctivaga	virescens	viridis	vlkianum
Habitat		estuarine	brackish	brackish	freshwater	brackish	marine	brackish	brackish	brackish	peat pools	littoral epilithic	brackish	marine and freshwater
Motile stage		strongly metabolic	ovate, compressed, with ventral depression, not metabolic	ovate-pyriform; slightly compressed	irregular, elongate, compressed strongly metabolic	irregular, elongate, compressed strongly metabolic	irregular, elongate, compressed strongly metabolic	irregularly broadly lobed elongate; slightly compressed; metabolic	elongate	compressed with ventral depression; not metabolic	elongate; not metabolic	elongate; somewhat metabolic	compressed with strong ventral depression	compressed with ventral depression
Non-motile stage		dominant stage, thick and striated mucilage, flagellar bases only present	not recorded	non motile cells recorded apparently having lost flagella	dominant stage, homogeneous mucilage, appendages not abbreviated	non motile cells recorded	homogeneous mucilage, appendages not abbreviated	recorded (no details published)	dominant stage, homogeneous mucilage, appendages incomplet	not recorded	dominant stage, stratified mucilage, appendages not abbreviated	homogeneous mucilage, appendages not abbreviated	not recorded	not recorded
Cell-size (µm)		5-6 x 3-4	6.5 (4.5-10) x 6.5 (5-9) x 2	5-9 (-13) x 4-5 x 2-3	6 (8-9) x 4.5 x 3.5-4	4-10 x 3-6 x 2-2.5	5-8 x 3-4	5-6 (-9) x 3.5-6 x 2.5-3	6-9 x 3-4.5	7-9 x 5-7 x 3-4	8 (5-12) x 6-8 x 4-5	7-8 x 2-3	6 x 4.8 x 4	3.5-7.5 x 4-5 x 1.5-3
Pseudopodia		-	+	+	+	+	+	+	-	-	-	-	-	+
Body-scales size (µm) and form		-	approx. 0.1 clavate	0.04 x 0.02 clavate	0.015 spherical	0.01 spherical	-	-	-	0.015-0.02 spherical	-	-	-	-
Insertion of appendages		ventral in a depression	ventral in a depression	ventral in a depression	sub-apical in a depression	sub-apical	sub-apical	ventral in a depression	semi-ventral	semi-ventral	sub-apical	sub-apical	semi-ventral in a depression	ventral in a depression
Short (posterior) flagellum length (µm) and other comments		5-7, distal necklace of pearl is present	vestigial	approx. 0.2 vestigial	approx. 6	approx. 3	approx. 4	1-2	5	2-4	2.5 - 6	5	vestigial	4, accessory axoneme structures present
Long (anterior) flagellum	Length (µm)	7-12	17-20	12-17	10-20	6-20	8-11	6-10	10-13	5-11	6-18	13	9-12	7-10
	Hairs	long and fine	?	long and fine	long and fine	long and fine	long and fine	long and fine	long and fine	long and fine	long and fine	long and fine	long and fine	long and fine
	"Knob-scales" size (µm) and form	-	0.08 x 0.02 double constriction	0.05 x 0.02 double constriction	0.03 x 0.025 constricted	0.03 x 0.02 constricted	0.03 x 0.02 constricted	approx. 0.02 stellate	0.4 spherical	0.;02 spherical	0.05 x 0.03 clavate	0.025 x 0.03 muriform	0.02 x 0..3 spherical	-
	Arrangement of scales	-	?	regular	regular	regular	regular	?	regular	irregular	irregular	irregular	?	-
Haptonema length (µm)		1-2	4-5(-6)	2-4.5	2.5	1.5	approx. 2	approx 1	2	approx. 1	1.5-2.5	2-4	0.75	1
Plastid	Characteristics	1 yellow-brown parietal, ventral	1(-2) brown/ yellow markedly lobed	1-2 yellow-green	1 golden brown	1 golden brown	1 golden brown	1 pale yellow-green 4 lobes from dorsal isthmus	1 yellow-green parietal	1 yellow-green	1-2 brown	2 yellow-green	1 green	1 yellow/ green
	Arrangement of thylakoïds	parallel and helicoïdal	parallel and helicoïdal	parallel and helicoïdal	simply parallel	simply parallel	simply parallel	simply parallel	parallel with large inter-lamellar spaces	simply parallel	simply parallel	parallel with granum-like arrangement	simply parallel	simply parallel
	Pyrenoid	ventral, near flagellar insertion, bulging	1 per plastid on the inner face	-	posterior-bulging	posterior-bulging	posterior-bulging	-	-	-	-	-	-	-
	Stigma	osmiophilic vesicles present at transition between chloroplast and thylakoid stromata	-	-	apparent on the inner face of the plastid, associated with a pit	apparent on the inner face of the plastid, associated with a pit	apparent on the inner face of the plastid, associated with a pit	on the external face of the plastid	-	on the external face of the plastid	on the external face of the plastid	-	-	on the external face of the plastid

(- = absence, ? = no data)

listed culture collections. Marine species were grown in ES-Tris medium (Cosson 1987) and the freshwater species in modified Lefevre-Czarda medium (PavED) with peat extract prepared like the soil extract in ES-Tris and added at 1%. Temperature was 20 °C and illumination provided by day light fluorescent tubes at a photon flux of 30 μmol of photons.m^{-2}.s^{-1} and a light/dark cycle 12/12 h.

Microscopy: Light microscope observations were conducted with an Olympus BX51 (Olympus Corporation, Tokyo, Japan) equipped with differential interference contrast (DIC) optics. Whole mounts were prepared for TEM from a drop of culture fixed with 1% osmium vapour on a Formvar-coated grid and negative stained with 1% uranyl acetate diluted in water/ethanol (1:1). The samples were analysed with a Jeol 1011 transmission electron microscope (JEOL Ltd, Tokyo, Japan). For SEM, cells were mounted by sedimentation on thermanox cover slides treated with L-polylysine and then fixed with 4% glutaraldehyde in 0.1 M cacodylate buffer (pH 7.4) and 0.25 M sucrose. After stepwise dehydration in a graded alcohol series, the cells were critical point dried (Jeol Ltd, Tokyo, Japan) and finally coated with a thin layer of gold/palladium (Leica Microsystems GmbH, Wetzlar, Germany). Observations were made with a Jeol JSM 6400F SEM. TEM preparations for ultrastructural study were performed with a 2 hour 4% glutaraldehyde fixation in 0.1 M cacodylate buffer (pH 7.4) and 0.25 M sucrose at 4 °C. The fixed cells were washed with decreasing sucrose concentrations and then post fixed in 2% osmium tetroxide for 2 hours at 4 °C. After washing, the cells were embedded in 1% low melting point agar, dehydrated in a graded alcohol series and then impregnated in 1:1 Epon/ethanol for 30 min, 100% Epon for 30 min and 100% Epon overnight. Then cells were embedded in epon resin (Epon 812, EMS, Hatfield, United Kingdom) and polymerised for 24 h at 60 °C. Thin sections were cut with a diamond knife (Diatome) on a Leica microtome (Leica Microsystems GmbH, Wetzlar, Germany) and stained with 1% uranyl acetate for 15 min followed with Reynolds lead citrate for 5 min (Reynolds 1963). The sections were observed with a Jeol 1011 transmission electron microscope.

DNA extraction: Cultures of cells were harvested by centrifugation (4500 g, 15 min), washed twice with TE buffer, and suspended in 10 ml of lysis buffer (Tris, 0.1 M; EDTA, 0.05 M; NaCl, 0.1 M; 1% SDS; 2% N-lauroylsarcosine, proteinase K 200 mg/mL, pH 8.0) and incubated at 55 °C for 2 h for total DNA extraction. DNA was then extracted with equal volumes of phenol and chloroform and precipitated with ethanol (Maniatis et al. 1982).

Amplification of the SSU and LSU rDNA and intergenic regions: Primers used in this study for the PCR amplification are listed in Table 3. Due to difficulties to amplify the SSU in one step two additional internal primers were designed allowing the deduction of the complete SSU rDNA sequences. Standard PCR cycles were performed for the PCR amplification of the SSU and LSU rDNA and the intergenic regions as follow: a first denaturing step at 95 °C for 5 min followed by 30 cycles: 1 min. at 95 °C, 1 min. at 50 °C and 1 min. at 72 °C with a final extension at 72 °C for 5 min. Most of the amplification products were cloned in the commercial cloning vector pCR 4-TOPO (TOPO TA Cloning Kit; Invitrogen Corporation, Carlsbad, USA). Plasmids from positive colonies were purified with the QIAprep Spin Miniprep Kit (QIAGEN, Hilden, Germany). The cloned PCR products included in the plasmids were sequenced with the M13 primers in both directions.

Phylogenetic analysis: For SSU rDNA analyses, sequences obtained in this study were aligned together. Alignment was first obtained using the online version of the multiple alignment program MAFFT (http://align.bmr.kyushu-u.ac.jp/mafft/software, Katoh et al. 2007), and were then improved by hand using the sequence editor BIOEDIT (Hall 1999). Very variable regions were automatically removed using the Gblocks software (http://www1.imim.es/~castresa/Gblocks/Gblocks.html), with optimised parameters for rRNA alignments (minimum length of a block, 5; allowing gaps in half of positions). The Gblock software retained 1711 positions for phylogenetic analyses from the initial 1820 positions for the SSU rDNA and retained 729 positions from the initial 890 positions for the LSU rDNA. The most appropriate model of DNA substitution and associated parameters were estimated by three statistics based on the Akaike information criterion (AIC, Akaike 1974), AIC, AICc and BIC using MrAIC (Nylander 2004). A GTR distribution model was selected by taking into account a gamma-shaped distribution of the rates of substitution among sites (G) with the proportion of invariable sites (I) for both SSU and LSU rDNA gene analyses (GTR+G+I). The selected model and parameters were used to perform phylogenetics analyses. Phylogenetic trees were determined from both rDNA sequences (single and concatenated) by two phylogenetic methods: maximum likelihood (ML) using TREEFINDER (Jobb et al. 2004) and Bayesian analysis with Mr. Bayes v3.1.2 (Ronquist and Huelsenbeck 2003). The robustness of the branching of trees was tested by bootstrapping for the maximum likelihood inference and bootstrap values were based on 1000 replicates. Bayesian analysis was conducted with two runs of four Markov chains, for at least 5 000 000 generations, sampling every 100th generation. From the 50 000 trees found, 25% were discarded (time required for likelihood to converge on stationary value) by setting the burn-in option.

Pigment analyses: Cells of the strains indicated in Table 1 were harvested during the logarithmic phase of growth by gentle vacuum filtration onto 25-mm GF/F Whatman (Kent, UK) glass fibre filters and stored frozen (-80 °C) until analysis. Extraction and HPLC analysis of pigments was performed as described in Van Lenning et al. (2003). Pigment analyses were performed with a Thermo Separation Products chromatograph (currently Thermo Finnigan, San Jose, CA, USA), comprising a model P2000 solvent module, a UV3000 absorbance detector, an FL2000 fluorescence detector, an SN4000 controller, and a refrigerated (5 °C) A/S-3000 autosampler.

Acknowledgements

We are deeply indebted to all persons who collected samples, isolated strains and maintained cultures for several decades in laboratories. Without them this type of work could not have been possible. Bertrand Le Roy, as well as his predecessors, are sincerely thanked for their meticulous care in the maintenance of Algobank-Caen. Jacqueline Fresnel is thanked for her precious expertise in electron microscopy techniques. Pr Marie-Agnès Avenel of the Institut du Latin at the Université de Caen Basse-Normandie is warmly thanked for her critical assistance in the drafting of the diagnosis in Latin. We thank Yoann Canon, who attended the first work of this job in 2000. The ASSEMBLE

project (FP7-227799) funded some aspects of this work. The authors wish to dedicate this paper to Dr. Michael R. Droop, deceased on March 20, 2011, who discovered *Monochrysis lutheri*.

References

Akaike H (1974) A new look at the statistical model identification. IEEE Trans Autom Contr **19**:716–723

Billard C (1976) Sur une nouvelle espèce de *Pavlova*, *P. virescens* nov. sp. (Haptophycées). Soc Phycol de France Bull **21**:18–27

Billard C (1994) Life Cycles. In Green JC, Leadbeater BSC (eds) The Haptophyte Algae. The Systematics Association Special Volume 51. Oxford University Press, Oxford, pp 167–186

Butcher RW (1952) Contributions to our knowledge of the smaller marine algae. J mar biol Ass UK **31**:175–191

Cavalier-Smith T (1994) Origin and Relationships of Haptophyta. In Green JC, Leadbeater BSC (eds) The Haptophyte Algae. The Systematics Association Special Volume 51. Oxford University Press, Oxford, pp 413–436

Cavalier-Smith T (2002) The phagotrophic origin of eukaryotes and phylogenetic classification of Protozoa. Int J Syst Evol Microbiol **52**:297–354

Cosson J (1987) Croissance des sporophytes résultants d'hybridations interspécifiques et intergénériques chez les laminaires. Cryptog Algol **8**:61–72

Droop MR (1953) On the ecology of flagellates from some brackish and fresh-water pools of Finland. Acta Bot fenn **51**:3–52

Edvardsen B, Eikrem W, Green JC, Andersen RA, Moon-van der Staay ST, Medlin LK (2000) Phylogenetic reconstructions of the Haptophyta inferred from 18S ribosomal DNA sequences and available morphological data. Phycologia **39**:19–35

Fresnel J, Galle P, Gayral P (1979) Résultats de la microanalyse des cristaux vacuolaires chez deux Chromophytes unicellulaires marines: *Exanthemachrysis gayraliae*, *Pavlova* sp. (Prymnésiophycées, Pavlovacées). C R Acad Sc Paris **288**:823–825

Gayral P. (1980) Particularités et intérêt subséquent de la famille des Pavlovophycées (Chrysophycophytes, Prymnesiophycées). 105e Congrès national des Sociétés savantes III: 201–212.

Gayral P, Fresnel J (1979) *Exanthemachrysis gayraliae* Lepailleur (*Prymnesiophyceae*, *Pavlovales*): Ultrastructure et discussion taxinomique. Protistologica **XV**:271–282

Green JC (1973) Studies in the fine structure and taxonomy of flagellates in the genus *Pavlova*. II. A freshwater representative, *Pavlova granifera* (Mack) comb. nov. Br Phycol J **8**:1–12

Green JC (1975) The fine structure and taxonomy of haptophycean fagellate *Pavlova lutheri* (Droop) comb. nov. (= *Monochrysis lutheri* Droop). J mar biol Ass UK **55**:785–793

Green JC (1976) Notes on the flagellar apparatus and taxonomy of *Pavlova mesolychnon* van der Veer, and on the status of *Pavlova* Butcher and related genera within the *Haptophyceae*. J mar biol Ass UK **56**:595–602

Green JC (1980) The fine structure of *Pavlova pinguis* Green and a preliminary survey of the order *Pavlovales* (*Prymnesiophyceae*). Br Phycol J **15**:151–191

Green JC, Hibberd DJ (1977) The ultrastructure and taxonomy of *Diacronema vlkianum* (*Prymnesiophyceae*) with special reference to the haptonema and flagellar apparatus. J mar biol Ass UK **57**:1125–1136

Green JC, Hori T (1988) The fine structure of mitosis in *Pavlova* (*Prymnesiophyceae*). Can J Bot **60**:1497–1509

Green JC, Hori T (1994) Flagella and Flagellar Roots. In Green JC, Leadbeater BSC (eds) The Haptophyte Algae. The Systematics Association Special Volume 51. Oxford University Press, Oxford, pp 47–71

Green JC, Course PA, Tarran GA (1996) The life cycle of *Emiliania huxleyi*: A brief review and a study of relative ploidy levels analysed by flow cytometry. J Mar Systems **9**:33–44

Hall TA (1999) BioEdit: a user-friendly biological sequence alignment editor and analysis program for Windows 95/98/NT. Nucleic Acids Symp Ser **41**:95–98

Hori T, Green JC (1994) Mitosis and Cell Division. In Green JC, Leadbeater BSC (eds) The Haptophyte Algae. The Systematics Association special volume 51. Oxford University Press, Oxford, pp 91–109

Houdan A, Billard C, Marie D, Not F, Sáez AG, Young JR, Probert I (2004) Holococcolithophore-heterococcolithophore (Haptophyta) life cycles: flow cytometric analysis of relative ploidy levels. Syst Biodivers **1**:453–465

Jobb G, von Haeseler A, Strimmer K (2004) TREEFINDER: A powerful graphical analysis environment for molecular phylogenetics. BMC Evol Biol **28**:4–18

Kalina T (1970) *Corcontochrysis noctivaga* gen. et sp. n. (Chrysophyceae). Preslia **42**:297–302

Kalina T (1975) Taxonomie und ultrastruktur der art *Corcontochrysis noctivaga* (Haptophyceae). Preslia **47**:1–13

Katoh K, Kuma K, Toh H, Miyata T (2007) MAFFT version 5: improvement in accuracy of multiple sequence alignment. Nucleic Acids Res **33**:511–518

Kiss JZ, Triemer RE (1988) A comparative study of storage carbohydrate granules from *Euglena* (Euglenida) and *Pavlova* (Prymnesiida). J Protozool **35**:237–321

Klaveness D (1972) *Coccolithus huxleyi* (Lohmann) Kamptner. II. The flagellate cell, aberrant cell types, vegetative propagation and life cycles. Br Phycol J **7**:309–318

Lepailleur H (1970) Sur un nouveau genre de Chrysophycées: *Exanthemachrysis* nov. gen. (*E. gayralii* nov. sp.). C R Acad Sci **270**:928–931

Liu H, Aris-Brosou S, Probert I, de Vargas C (2010) A timeline of the environmental genetics of the haptophytes. Mol Biol Evol **27**:171–176

Liu H, Probert I, Uitz J, Claustre H, Aris-Brossou S, Frada M, Not F, de Vargas C (2009) *Haptophyta* rule the waves: Extreme oceanic biodiversity in non-calcifying haptophytes explains the 19-Hex paradox. Proc Natl Acad Sci USA **106**:12803–12808

Mack B (1954) Untersuchungen an Chrysophyceen V. –VIII. Österr Bot Z **101**:64–73

Maniatis T, Fritsch EF, Sambrook J (1982) Molecular Cloning, A Laboratory Manual. Cold Spring Harbor Laboratory Press, Cold Spring Harbor, New York

Medlin LK, Sáez AG, Young JR (2008) A molecular clock for coccolithophores and implications for selectivity of phytoplankton extinctions across the K/T boundary. Mar Micropaleontol **67**:69–86

Medlin L, Elwood HJ, Stickel S, Sogin ML (1988) The characterization of enzymatically amplified eukaryotic 16S-like rRNA-coding regions. Gene **71**:491–499

Meireles LA, Guedes AC, Malcata FX (2003) Lipid class composition of the microalga *Pavlova lutheri*: eicosapentaenoic and docosahexaenoic acids. J Agr Food Chem **51**:2237–2241

Moestrup Ø (1994) Economic Aspects: "Blooms", Nuisance Species, and Toxins. In Green JC, Leadbeater BSC (eds) The Haptophyte Algae. The Systematics Association Special Volume 51. Oxford University Press, Oxford, pp 265–285

Nosenko T, Boese B, Bhattacharya D (2007) Pulsed field gel electrophoresis analysis of genome size and structure in *Pavlova gyrans* and *Diacronema sp.* (Haptophyta). J Phycol **43**:763–767

Nylander JAA (2004) MrAIC.pl. Program distributed by the author. Evolutionary Biology Centre, Uppsala University

Ponis E, Probert I, Véron B, Le Coz J-R, Mathieu M, Robert R (2006) Nutritional value of six Pavlovophyceae for *Crassostrea gigas* and *Pecten maximus* larvae. Aquaculture **254**:544–553

Prauser H (1958) *Diacronema vlkianum*, eine neue Chrysomonade. Arch Protistenkd **103**:117–128

Reynolds ES (1963) The use of lead citrate at high pH as an electron-opaque stain in electron microscopy. J Cell Biol **17**:208–212

Ronquist F, Huelsenbeck JP (2003) MRBAYES 3: Bayesian phylogenetic inference under mixed models. Bioinformatics **19**:1572–1574

Shi XL, Marie D, Jardillier L, Scanlan DJ, Vaulot D (2009) Groups without cultured representatives dominate eukaryotic picophytoplankton in the oligotrophic South East Pacific Ocean. PLoS ONE **4(10)**:e7657, doi:10.1371/journal.pone0007657

Tonon T, Harvey D, Larson TR, Yi L, Graham IA (2005) Acyl-CoA elongase activity and gene from the marine microalga *Pavlova lutheri* (Haptophyceae). J Appl Phycol **17**:111–118

Tseng CK, Chen J, Zhang Z (1992) On a new species of *Pavlova* (*Prymnesiophyceae*) from China. Chin J Oceanol Limnol **10**:23–28

Vargas C de, Aubry MP, Probert I, Young J (2007) Origin and Evolution of Coccolithophores: From Coastal Hunters to Oceanic Farmers. In Falkowski PG, Knoll A (eds) Evolution of Primary Producers in the Sea. Elsevier, Academic Press, Amsterdam, Heidelberg, pp 251–285

Veer J van der (1969) *Pavlova mesolychnon* (*Chrysophyta*) a new species from the Tamar Estuary, Cornwall. Acta Bot Neerl **18**:496–510

Veer J van der (1972) *Pavlova helicata* (*Haptophyceae*), a new species from the Frisian Island Schiermonnikoog, the Netherlands. Nova Hedw **23**:131–159

Veer J van der (1976) *Pavlova calceolata* (*Haptophyceae*) a new species from the Tamar Estuary, Cornwall. J mar biol Ass UK **56**:21–30

Veer J van der (1979) Pavlova and the Taxonomy of Flagellates Especially the Chrysomonads. PhD Thesis, Rijks-universiteit, Groningen, The Netherlands.

Veer J van der, Leewis RJ (1977) *Pavlova ennorea* sp. nov. a haptophycean alga with a dominant non-motile phase from England. Acta Bot Neerl **26**:159–176

Van Lenning K, Estrada M, Latasa M, Medlin L, Probert I, Véron B, Sáez AG, Young J (2003) Pigment signatures and phylogenetic relationships of the *Pavlovophyceae* (*Haptophyta*). J Phycol **39**:379–389

Véron B, Dauguet J-C, Billard C (1996) Sterolic biomarkers in marine phytoplankton. I. Free and conjugated sterols of *Pavlova lutheri* (Haptophyta). Eur J Phycol **31**:211–215

Volkman JK, Farmer CM, Barrett SM, Sikes EL (1997) Unusual dihydroxysterols as chemotaxonomic markers for microalgae from the order *Pavlovales* (*Haptophyceae*). J Phycol **33**:1016–1023